https://doi.org/10.5194/egusphere-2024-3798
Preprint. Discussion started: 17 December 2024

A trait-based model to describe plant community dynamics in managed grasslands (GrasslandTraitSim.jl v1.0.0)

Felix Nößler[1], Thibault Moulin[1], Oksana Buzhdygan[1], Britta Tietjen[1,2], and Felix May[1]

[1]Institute of Biology, Freie Universität Berlin, Theoretical Ecology, Berlin, Germany
[2]Berlin-Brandenburg Institute of Advanced Biodiversity Research, Berlin, Germany

Correspondence: Felix Nößler (felix.noessler@fu-berlin.de)

Abstract. Temperate semi-natural grassland plant communities are expected to shift under global change, mainly due to land use and climate change. However, the interaction of different drivers on diversity and the influence of diversity on the provision of ecosystem services are not fully understood. To synthesise the knowledge on grassland dynamics and to be able to predict community shifts under different land use and climate change scenarios, we developed the GrasslandTraitSim.jl model. In contrast to previously published grassland models, we link morphological plant traits to species-specific processes via transfer functions, thus avoiding a large number of species-specific parameters that are difficult to measure and calibrate. This allows any number of species to be simulated based on a list of commonly measured traits: specific leaf area, maximum height, leaf nitrogen per leaf mass, leaf biomass per plant biomass, above-ground biomass per plant biomass, root surface area per below-ground biomass, and arbuscular mycorrhizal colonisation rate. For each species, the dynamics of the above- and below-ground biomass and its height are simulated with a daily time step. While the soil water content is simulated dynamically, the nutrient dynamics are kept simple, assuming that the nutrient availability depends on total soil nitrogen and the total plant biomass. We present a model description, which is complemented by online documentation with tutorials, flowcharts, and interactive graphics, and calibrate the model to grassland sites with different number of mowing events and grazing intensity in central Germany. Furthermore, we show how the model can be used to conduct simulation experiments to analyse shifts in plant community composition under different land use intensities. We believe that the GrasslandTraitSim.jl model is a useful tool for predicting plant biomass production and plant functional composition of temperate grasslands in response to management under climate change.

https://doi.org/10.5194/egusphere-2024-3798
Preprint. Discussion started: 17 December 2024

1 Introduction

Permanent semi-natural grasslands cover 30.5% of the agricultural area of the European Union (Eurostat, 2020) and many of them are known to support high levels of biodiversity (Petermann and Buzhdygan, 2021). At small spatial scales (< 100 m^2), extensively managed grasslands have the highest recorded plant species richness per area in the world (Wilson et al., 2012). These plant species-rich habitats can in turn support many other taxonomic groups, such as butterflies (European Environment Agency et al., 2013), which are adapted to open habitats. Moreover, 29% of the European bird species are associated with grassland habitats (Nagy, 2009). In conclusion, temperate grasslands can play a role in supporting biodiversity in agricultural landscapes.

The key factor in maintaining grasslands is management. Without management, grassland would become woodland because the abiotic conditions on most grassland sites are favourable to woodland growth, such as soils that are neither too dry nor too wet. Mowing and grazing influence the plant species composition of grasslands and prevent the encroachment of woody species. Therefore, grasslands and agriculture have been coevolving in Europe since the last glacial period (Hejcman et al., 2013; Pärtel et al., 2005). The intensity and type of land use influence the level of grassland biodiversity. Both intensification and abandonment can lead to a decline in grassland biodiversity (Gossner et al., 2016; Schils et al., 2020). Intensification, more specifically higher fertilization, more mowing events per year, and/or a higher livestock density leads to a dominance of a few fast-growing plant species that are adapted to the high disturbance frequency by mowing and grazing. Abandonment, on the other hand, leads to the growth of woody species and a loss of specialists of open habitats (Hilpold et al., 2018). Management is therefore a key driver of plant community composition in grasslands.

Furthermore, climate change is expected to shift the community composition of grasslands, particularly during heat waves and droughts (Griffin-Nolan et al., 2019; Schils et al., 2020). In addition, the community composition of grasslands affects the provision of ecosystem services, such as biomass production, resistance to climatic events, and pollination (Van Oijen et al., 2020). However, how different drivers and their interactions impact the community composition and how the composition relates to ecosystem service provision is poorly understood. In particular, the conditions under which a diverse plant community leads to higher biomass production remain a topic of debate (Adler et al., 2011; Chen et al., 2018; Dee et al., 2023). This highlights the need for a more comprehensive mechanistic understanding of the underlying processes. Simulation models can complement experimental and observational studies to predict the effects of management and climate change on grassland community dynamics and ecosystem service provision, and can help provide a better mechanistic understanding of processes. Current scientific knowledge is integrated into the models, and the models can be used to test hypotheses and to generate new knowledge (Clark et al., 2001; Jeltsch et al., 2008). Dynamic simulation models are therefore a useful tool for disentangling the effects of land use and climate on the plant community composition and the provision of ecosystem services by grasslands.

Historically, different research questions on grasslands, ranging from ecology to biogeochemistry, have led to the development of different grassland models by focusing on different parts of the model and simplifying other parts. In ecology, for example, questions about plant coexistence in grasslands have led to models with a strong focus on species interactions. In the biogeochemical community, for example, questions were asked about the emission of greenhouse gases from grasslands,

https://doi.org/10.5194/egusphere-2024-3798
Preprint. Discussion started: 17 December 2024

leading to the development of models with a focus on biogeochemical cycles in grasslands (Van Oijen et al., 2018). Ecological models are often simpler models and can be divided into difference or differential equation models and individual-based models. While individual-based models are characterised by a bottom-up approach by modelling the interactions of individuals, difference/differential equation models are characterised by a top-down approach by modelling the interactions of species, leading in both cases to the emergence of grassland community patterns. Examples of individual-based models are IBC-grass (May et al., 2009), originally developed to analyse the effects of grazing on plant communities, and GRASSMIND (Taubert et al., 2012), which can simulate the effects of climate change, mowing, fertilisation and irrigation on plant community dynamics. Examples of ecological differential equation models are DynaGraM (Moulin et al., 2021) and GraS (Siehoff et al., 2011), both of which can simulate the effect of mowing and grazing on the plant community. There are also more theoretical models that follow the Lotka-Volterra differential equations to simulate grassland dynamics (Geijzendorffer et al., 2011; Fort, 2018; Pulungan et al., 2019; Chalmandrier et al., 2021). Competition between plant species is included in these models with interaction coefficients. The way species or plant functional types are represented in all these models differ. The plant functional types in IBC-grass are determined by categories of growth forms, maximum plant size, resource response and grazing response and GRASSMIND by morphological and physiological traits. GraS represents species by species indicator values and in DynaGraM species are represented by a combination of morphological and physiological traits and parameters derived from species indicator values. While IBC-grass, GraS and the models using Lotka-Volterra type equations focus strongly on ecological issues and are weak in representing biogeochemical cycles, GRASSMIND is coupled with a soil model and DynaGram has a basic representation of nutrient and water cycles included. In contrast, models developed by the biogeochemical scientific community have a thorough representation of the nutrient, water and carbon cycles in grasslands (Van Oijen et al., 2020). Examples include PaSim (Riedo et al., 1998), LPJmL (Rolinski et al., 2018) and CENTURY/DayCent (Parton, 1996; Parton et al., 1998). Recently, progress has been made to improve the representation of plant functional diversity in biogeochemical grassland models (Movedi et al., 2019; Wirth et al., 2024). In summary, existing grassland models vary in their complexity in representing plant diversity and biogeochemical cycles, and in how species are represented: by species indicator values, trait categories, morphological traits and/or physiological traits.

Modelling multi-species assemblages in grasslands has been identified as one of the key challenges in grassland modelling (Kipling et al., 2016). This is due to the fact that process-based grassland models require data on the physiological and demographic processes of species, such as measurements of growth rates of species under different radiation intensities. As demographic and physiological data are not readily available for many species, the number of species that can be modelled is limited (Jeltsch et al., 2008; Chalmandrier et al., 2021). To overcome the problem of missing demographic and physiological data, measurable morphological trait data can be used instead. Morphological trait data can be measured more easily and are available for many plant species, for example from the plant trait database TRY (Kattge et al., 2020). For many morphological traits, it is known from experimental and observational studies how they affect species-specific processes. For example, a high specific leaf area is associated with high photosynthetic activity per leaf mass and a high senescence rate (Wright et al., 2004). Here, we use exac his approach of linking morphological trait species-specific processes to develop the process-based model GrasslandTraitSim.jl. model is partly based on the DynaGraM model (Moulin et al., 2021), which in turn is based

https://doi.org/10.5194/egusphere-2024-3798
Preprint. Discussion started: 17 December 2024

on LINGRA (Schapendonk et al., 1998) and ModVege (Jouven et al., 2006), but is now able to simulate any number of species, as we used 70 species in our simulations, and is more suitable for analysing changes in the community trait composition. To our knowledge, the simulation of species-rich assemblages has not been done before in process-based grassland models of intermediate complexity (for simpler models see e.g. Pulungan et al., 2019; Chalmandrier et al., 2021). One exception is the IBC-grass model, which has a similar level of complexity, but uses discrete trait categories (e.g. small, medium and large maximum plant size; May et al., 2009). In IBC-grass the large number of species is created by using all combinations from the trait categories. We argue that we have a more realistic representation of species by using continuous traits from real species as inputs. Therefore, we believe that our GrasslandTraitSim.jl model can fill a gap in existing grassland simulation models for simulating multi-species assemblages and predicting the functional composition of plant communities in grasslands in response to management and climate change. As plant functional composition influences biomass supply in the model, cascading effects from management and climate through plant functional composition to biomass supply can be analysed. We will present a comprehensive model description, calibration to managed grassland sites in Germany and demonstrate how the model can be used to study the effects of management on grassland community dynamics.

https://doi.org/10.5194/egusphere-2024-3798
Preprint. Discussion started: 17 December 2024

2 Description of the GrasslandTraitSim.jl model

The GrasslandTraitSim.jl model is designed to simulate the dynamics of grassland communities under different management scenarios, soil and climatic conditions. The model is run on daily time steps (indicated by the t subscript) and the spatial resolution is per patch (indicated by the x and y subscripts), allowing the use of spatially heterogeneous inputs. Within each patch, many plant species (denoted by the subscript s) can grow. The model has four types of state variables: above-ground dry biomass $B_{A,txys}$ [$\mathrm{kg \cdot ha^{-1}}$], below-ground dry biomass $B_{B,txys}$ [$\mathrm{kg \cdot ha^{-1}}$], height H_{txys} [m], and soil water content in the rooting zone W_{txy} [mm] (Fig. 1). The sum of the above-ground and below-ground dry biomass equals the total dry biomass B_{txys} [$\mathrm{kg \cdot ha^{-1}}$]. Changes in the state variables are described by a set of coupled difference equations (for an overview see Table B3). The morphological functional traits of all plant species are fixed (time-invariant inputs) and linked by model parameters to the species' demographic processes (Fig. 2). As a result of the differences in the demographic rates of all species, the performance of individual plant species differs, leading to the emergence of plant community dynamics. While reading the model description, we encourage the reader to take a look at the online documentation, which contains many interactive graphics and flowcharts (see data accessibility statement).

The required input variables are the plant functional traits of each species, soil properties, daily climatic data and daily management data (Table B1). The model has in total 51 global parameters that are neither site, time nor species dependent (see Table B2). Outputs include the state variables, grazed and mown biomass, community-weighted mean and variance of each trait, taxonomic diversity indices (e.g. Simpson diversity), and plant functional diversity indices (e.g. Functional dispersion and Functional evenness) and can be calculated for each day and patch. Users can choose to provide spatially heterogeneous inputs. However, there is currently no interaction between patches and it is possible to run simulations with just one patch. The simulation is not affected by the patch size. Nevertheless, it is useful to be aware of the patch size for which the model was designed. The patch size that we consider reasonable is between 1 $\mathrm{m^2}$ and 1 ha. If we consider a small resolution for the patch size, we can assume that plants are competing for the same resources and therefore directly affecting each other. However, if we consider a larger patch size, an average competition between plants is simulated.

The model procedure is divided into an initialisation and a simulation part. During initialisation, the initial biomass, which is 5000 $\mathrm{kg \cdot ha^{-1}}$ by default, is divided equally between all species and split between above-ground and below-ground biomass according to the trait above-ground biomass per total biomass abp_s [$-$]. The initial soil water content is set to 180 mm by default. Height is set to half the maximum height $maxheight$ [m] trait of the species. During the simulation, a loop is run over each day over each patch. Very low or negative values ($< 10^{-30}$) of the height H_{txys} and biomass state variables (B_{txys}, $B_{A,txys}$, and $B_{B,txys}$) are set to zero to avoid numerical problems. After that, the main part of the model is executed in the following order: growth (Eqs. 5-34), senescence (Eqs. 35-36), management (Eqs. 37-43), height dynamics (Eq. 44), and soil water dynamics (Eqs. 45-53). However, the order of the execution has no influence on the results, because the change of the state variables is calculated based on forcing variables (input variables) of the day and state variables of the previous day.

https://doi.org/10.5194/egusphere-2024-3798
Preprint. Discussion started: 17 December 2024

2.1 Biomass dynamics

The change in the total biomass B from day t to $t+1$ of species s in patch x, y [$\mathrm{kg \cdot ha^{-1}}$] is calculated based on the actual growth $G_{act,txys}$ [$\mathrm{kg \cdot ha^{-1}}$] (Eq. 5), and the losses by senescence S_{txys} [$\mathrm{kg \cdot ha^{-1}}$] (Eq. 35) and management M_{txys} [$\mathrm{kg \cdot ha^{-1}}$] (Eq. 37):

$$B_{t+1xys} = B_{txys} + G_{act,txys} - S_{txys} - M_{txys} \tag{1}$$

The change in the total biomass B_{txys} is divided into the change in above-ground $B_{A,txys}$ [$\mathrm{kg \cdot ha^{-1}}$] and below-ground biomass B_{txys} [$\mathrm{kg \cdot ha^{-1}}$]. We assume that plants aim to achieve a similar level of above-ground biomass per total biomass similar to the time-invariant trait above-ground biomass per total biomass abp_s [$-$]. We therefore calculate A_{txys} [$-$] the ratio between the actual biomass ratio and the trait abp_s:

$$A_{txys} = \frac{\left(\frac{B_{A,txys}}{B_{txys}}\right)}{abp_s} \tag{2}$$

A_{txys} is less than one if the above-ground biomass per total biomass is less than expected by the trait abp_s, for example after a mowing event. This variable can be used to allocate biomass changes by growth and senescence to above-ground and below-ground biomass. Biomass loss by mowing and grazing affects only the above-ground biomass:

$$B_{A,t+1xys} = B_{A,txys} + A_{txys} \cdot G_{act,txys} - (1 - A_{txys}) \cdot S_{txys} - M_{txys} \tag{3}$$

$$B_{B,t+1xys} = B_{B,txys} + (1 - A_{txys}) \cdot G_{act,txys} - A_{txys} \cdot S_{txys} \tag{4}$$

This formulation allows for rapid regrowth of above-ground biomass after a grazing period or a mowing event, as little of the growth is allocated to below-ground biomass and most is allocated to above-ground biomass.

The actual growth is derived from the community potential growth $G_{pot,txy}$ [$\mathrm{kg \cdot ha^{-1}}$] (Eq. 6) and the multiplicative effect of five growth adjustment factors:

$$G_{act,txys} = G_{pot,txy} \cdot LIG_{txys} \cdot NUT_{txys} \cdot WAT_{txys} \cdot ROOT_{txys} \cdot ENV_{txy} \tag{5}$$

where LIG_{txys} [$-$] is the species-specific competition for light (Eq. 11), NUT_{txys} [$-$] is the species-specific competition for nutrients (Eq. 16), WAT_{txys} [$-$] is the species-specific competition for soil water (Section 2.1.5), $ROOT_{txys}$ [$-$] is the species-specific cost for maintaining roots and mycorrhiza (Eq. 27), and ENV_{txy} [$-$] is the non-species-specific adjustment based on environmental and seasonal factors (Eq. 30).

2.1.1 Community potential growth

The model follows the concept of the light use efficiency (Monteith, 1972) that describes how much dry matter the plants can build based on the solar radiation. This concept was widely adopted in grassland modelling studies (Schapendonk et al., 1998; Jouven et al., 2006; Moulin et al., 2021) for view see Pei et al. (2022). The community potential growth $G_{pot,txy}$ is

https://doi.org/10.5194/egusphere-2024-3798
Preprint. Discussion started: 17 December 2024

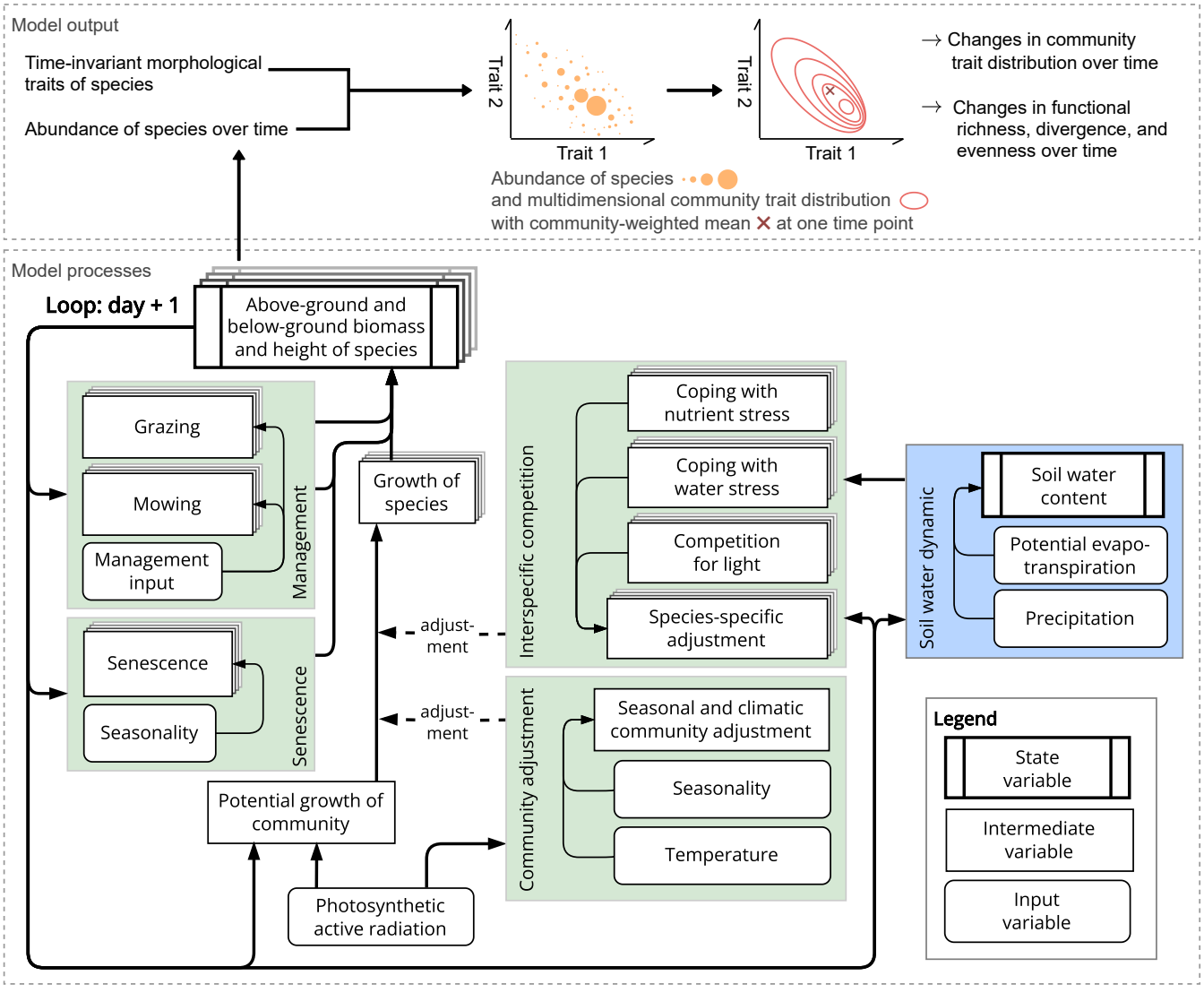

Figure 1. Structure of the GrasslandTraitSim.jl model for one patch. Boxes represent state, intermediate, and input variables (forcing functions), and arrows indicate the influence of one variable on another. We use the term intermediate variables to describe variables that are neither inputs nor state variables, but are important intermediate results in the calculation of the change in state variables. While the green areas show calculations that influence the change in above- and below-ground biomass and height, the blue area shows the calculation of the change in soil water content in the rooting zone. The arrows originating from the biomass and height of the species indicate that both the biomass and height play a role in the processes outlined in the green and blue areas. However, for simplicity, they do not indicate the exact position within the areas. Species-specific variables are represented by a series of offset boxes positioned behind one another, indicating the presence of multiple species within the model. We show how the distribution of community traits can be calculated from the model output; other model outputs include the state variables and the grazed and mown biomass, which can be summarised at the community level.

https://doi.org/10.5194/egusphere-2024-3798
Preprint. Discussion started: 17 December 2024

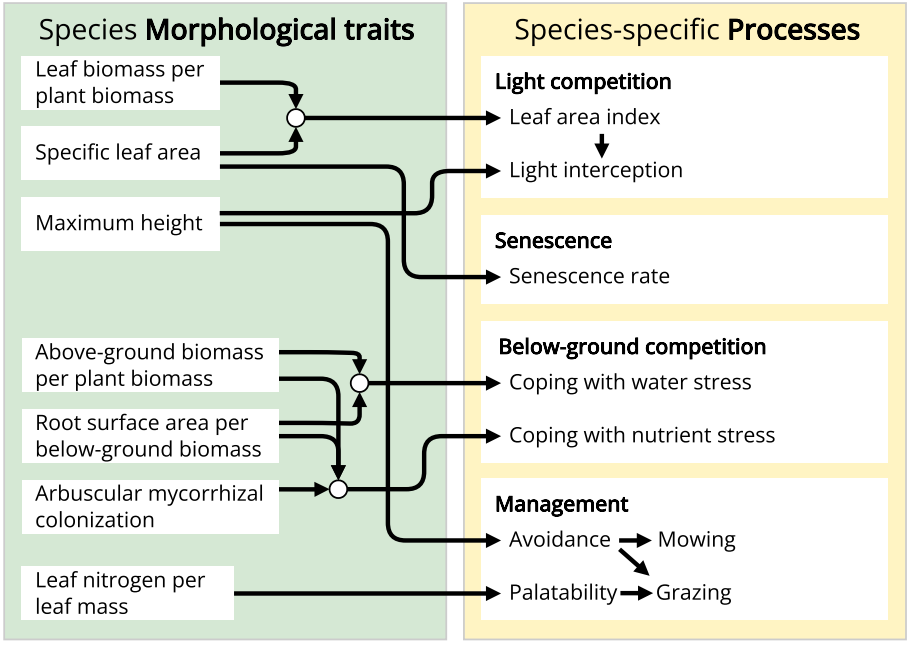

Figure 2. The GrasslandTraitSim.jl model links morphological plant functional traits to processes. Arrows indicate which process or variable is influenced by each plant functional trait. Each plant functional trait can have species-specific values, allowing for species-specific responses in many of the model's processes.

described by:

$$G_{pot,txy} = PAR_{txy} \cdot \gamma_{RUEmax} \cdot FPAR_{txy} \tag{6}$$

with the photosynthetic active radiation PAR_{txy} [$\mathrm{MJ} \cdot \mathrm{ha}^{-1}$], maximal radiation use efficiency γ_{RUEmax} [$\mathrm{kg} \cdot \mathrm{MJ}^{-1}$], and the fraction of PAR_{txy} that is intercepted by the plants $FPAR_{txy}$ [$-$].

The modelled fraction of radiation intercepted by the plants is determined by the number of leaves and the height of the community. A saturation function is used to describe the relationship between leaf area per ground area (leaf area index) and light interception. We argue that light interception is less effective when all plants are rather short, because the leaves are more densely packed. Individual plants avoid shading by growing taller (Heger, 2016). Therefore, we include the height of the community in the light interception calculation, also to prevent that a community with short plants can build up a very high biomass. More technically, we use the Beer-Lambert equation to model the non-linear response of the fraction of light intercepted $FPAR_{txy}$ to the total leaf area index $LAI_{tot,txy}$ (Monsi, 1953; Monsi and Saeki, 2005). This relationship is governed by the light extinction coefficient $\gamma_{RUE,k}$ [$-$], which determines how quickly the fraction of absorbed radiation approaches one as the leaf area index increases. Reduction of radiation use efficiency because of densely packaged leaves is a function of the community-weighted mean height and influenced by the parameter $\alpha_{RUE,cwmH} \in [0, 1]$ [$-$], which specifies the growth reduction at $H_{cwm,txy} = 0.2\mathrm{m}$. The parameter has been arbitrarily set to the reference height of 0.2 m because it

https://doi.org/10.5194/egusphere-2024-3798
Preprint. Discussion started: 17 December 2024

is easier to think about the growth reducer for a specific height. If $H_{cwm,txy}$ is greater than 0.2 m, less self-shading will occur because the leaves are less densely packed and therefore the growth reduction is less than $\alpha_{RUE,cwmH}$:

$$FPAR_{txy} = (1 - \exp(-\gamma_{RUE,k} \cdot LAI_{tot,txy})) \cdot \exp\left(\frac{\log(\alpha_{RUE,cwmH}) \cdot 0.2\text{m}}{H_{cwm,txy}}\right) \tag{7}$$

with the community-weighted mean height, calculated by weighting the height H_{txys} [m] of each species by its share of above-ground biomass $B_{A,txys}$ of the total above-ground biomass $B_{totA,txy}$ [$\text{kg} \cdot \text{ha}^{-1}$]:

$$H_{cwm,txy} = \sum_{s=1}^{S} \frac{B_{A,txys}}{B_{totA,txy}} \cdot H_{txys} \tag{8}$$

The total leaf area index $LAI_{tot,txy}$ is the sum of the species-specific leaf area indices LAI_{txys}:

$$LAI_{tot,txy} = \sum_{s=1}^{S} LAI_{txys}, \tag{9}$$

where LAI_{txys} is defined as

$$LAI_{txys} = B_{A,txys} \cdot sla_s \cdot \frac{lbp_s}{abp_s} \cdot 0.1, \tag{10}$$

with above-ground biomass $B_{A,txys}$ [$\text{kg} \cdot \text{ha}^{-1}$], specific leaf area sla_s [$\text{m}^2 \cdot \text{g}^{-1}$], leaf biomass per plant biomass lbp_s [$-$], above-ground biomass per total biomass abp_s [$-$]. As $B_{A,txys}$ and sla_s must be converted to the same unit, Eq. 10 is multiplied by 0.1.

2.1.2 Species-specific light competition

We have shown how to calculate the potential growth of the community based on the total leaf area index and community height, now we want to distribute the growth to the plant species based on their leaf area index and height. Species with a higher leaf area index can incept more light and taller species receive greater light exposure and are less affected by shading from other plant species. The leaf area index of the species considers that plant species which transfer more biomass to their leaves, and have thinner leaves, can build a greater leaf area. This allows them to use the photosynthetic active radiation more efficiently. Being overtopped by other plants or investing more in supporting tissue and less in leaves is a common trade-off in plant strategies (Westoby et al., 2002). We employ two different methods of varying complexity for the light competition and the user can choose which method to use.

The first method is simpler and less computationally demanding and takes into account the leaf area index ratio and the height of the species. More solar radiation is allocated to plants whose height H_{txys} [m] is greater than the community-weighted mean height $H_{cwm,txy}$ [m] (see Eq. 8). The parameter $\beta_{LIG,H}$ [$-$] controls how much the plant height affects the distribution of solar radiation. If $\beta_{LIG,H}$ is zero, the distribution of solar radiation to plant species is solely influenced by the ratio of the leaf area index of the species LAI_{txys} to the total leaf area index $LAI_{tot,txy}$. The sum of all species-specific light competition factors LIG_{txys} is equal to one:

$$LIG_{txys} = \frac{LAI_{txys} \cdot (H_{txys}/H_{cwm,txy})^{\beta_{LIG,H}}}{\sum_{i=1}^{S} LAI_{txyi} \cdot (H_{txyi}/H_{cwm,txy})^{\beta_{LIG,H}}} \tag{11}$$

https://doi.org/10.5194/egusphere-2024-3798
Preprint. Discussion started: 17 December 2024

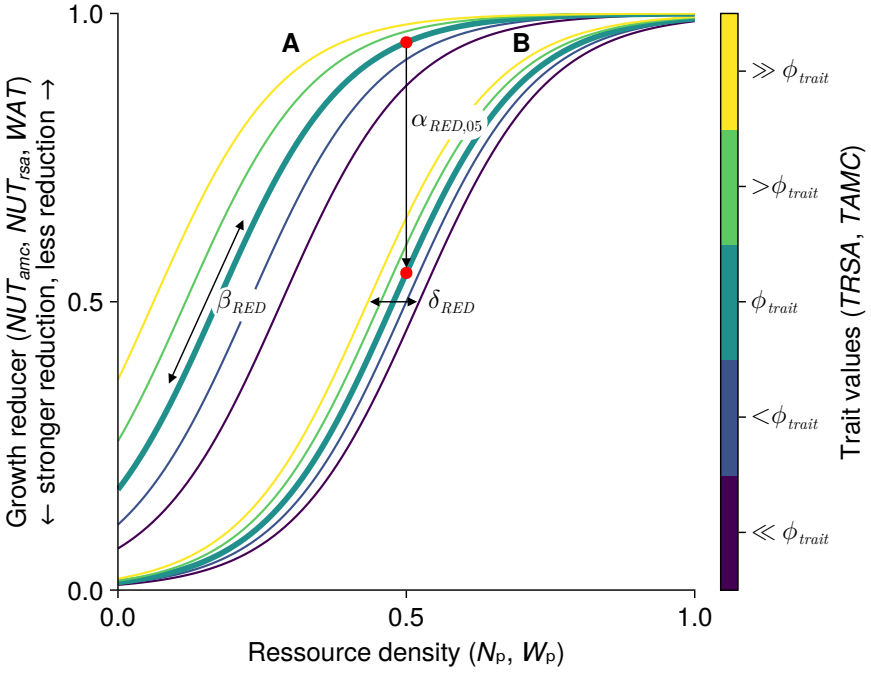

Figure 3. General form of growth reducer as a function of resource density (plant available nutrients and soil water). The function is governed by the four parameters β_{RED} (slope of the logistic function), ϕ_{trait} (usually the mean trait value), $\alpha_{RED,05}$ (growth reduction at half the resource density for species with a trait value of ϕ_{trait}, marked by a red dot), and δ_{RED} (controls how much the species-specific inflection points differ from the inflection point of a species with value of ϕ_{trait}). We show two different curves for different parameter values: A with $\alpha_{RED,05} = 0.95$ and $\delta_{RED} = 0.25$; B with $\alpha_{RED,05} = 0.55$ and $\delta_{RED} = 0.1$. In both cases we used $\beta_R = 9$, $\phi_{trait} = 20$ and the trait values 16, 18, 20, 22 and 24 (from dark purple to yellow). We include dynamic versions with sliders for the parameters for the three growth reducers $NUT_{amc,txys}$, $NUT_{rsa,txys}$, and WAT_{txys} in the supplementary material (see data accessibility statement).

In the second method, we derive the proportion of light intercepted by each species out of the total light intercepted by dividing the sward into vertical height layers of constant width, by default 0.05 m, to account for shading (similar to Taubert et al., 2012). We want to calculate how much light is intercepted in each height layer l $INT_{txy,l}$ $[-]$. Therefore, we need to calculate how much light is intercepted in the layers above and the interception in layer l. We assume that the biomass, and therefore also the leaf area index, is uniformly distributed over the height of the plant. Thus, we can calculate the leaf area index of each species in each height layer $LAI_{txys,l}$ $[-]$ and the total leaf area index of all species in each layer $LAI_{tot,txy,l}$ $[-]$. For each layer we can calculate the total leaf area index above the layer up to the maximum height layer L. The maximum height layer can be reached by the tallest plants with the highest $maxheight$ $[\mathrm{m}]$. The reduction in incoming light based on the total leaf area index of the layers above and the interception of layer l is used to calculate the proportion of light intercepted in

https://doi.org/10.5194/egusphere-2024-3798
Preprint. Discussion started: 17 December 2024

layer l $INT_{txy,l}$:

$$INT_{txy,l} = \exp\left(\gamma_{RUE,k} \cdot \sum_{z=l+1}^{L} LAI_{tot,txy,z}\right) \cdot (1 - \exp(\gamma_{RUE,k} \cdot LAI_{tot,txy,l})) \tag{12}$$

The proportion of light intercepted in the layer can be used to obtain the proportion of light intercepted for each species in each layer by multiplying $INT_{txy,l}$ by the leaf area index proportion of the layer. The sum of all species-specific light interception proportions across all layers can be used to calculate the light competition factor LIG_{txys} [−]:

$$LIG_{txys} = \sum_{z=l}^{L} INT_{txy,l} \cdot \frac{LAI_{txys,z}}{LAI_{tot,txy,z}} \cdot \frac{1}{1 - \exp(\gamma_{RUE,k} \cdot LAI_{tot,txy})} \tag{13}$$

We divide the term by the total interception of all layers (compare Eq. 7) to ensure that the sum of all species-specific light competition factors is equal to one. The parameter $\beta_{LIG,H}$ is not used in this method.

2.1.3 General form of the growth reducer for nutrient and water stress

We use the same equations with different parameters to relate the plant-available nutrients and plant-available soil water to the growth reducers of nutrient and water stress. Therefore, we show here the general form of the equations (see Fig. 3) to avoid repetition and define the specific variables and parameters used in the next two sections on nutrient and water stress. The derivation of the equations is shown in more detail in Appendix A. We use a logistic function to relate the resource density R_{txy} (general symbol for the plant-vailable nutrients $N_{p,txys}$ and the plant-available water $W_{p,txy}$) to the growth reducer RED_{txys} (general symbol for the growth reducers for nutrients stress $NUT_{amc,txys}$ and $NUT_{rsa,txys}$ and water stress WAT_{txys}). The growth reducer RED_{txys} lies between zero (no growth possible) and one (no growth reduction at all). While the inflection points of the logistic function $x_{0,RED,txys}$ (general symbol for $x_{0,NUT,rsa,s}$, $x_{0,NUT,amc,s}$, and $x_{0,WAT,s}$) are species-specific depending on the trait values $trait_{txys}$ (general symbol for the root surface area per total biomass $TRSA_{txys}$ and the arbuscular mycorrhizal colonisation rater per total biomass $TAMC_{txys}$), the slope β_{RED} (general symbol for $\beta_{NUT,rsa}$, $\beta_{NUT,amc}$, and $\beta_{WAT,rsa}$) is not species-specific. We assume that if the plant has a trait value equal to the parameter ϕ_{trait} (general symbol for ϕ_{TRSA} and ϕ_{TAMC}), then the growth reduction at 0.5 resource density is $\alpha_{RED,05}$ (general symbol for $\alpha_{NUT,rsa,05}$, $\alpha_{NUT,amc,05}$, and $\alpha_{WAT,rsa,05}$). The parameter ϕ_{trait} can be set to the mean trait of a community, then the parameter $\alpha_{RED,05}$ can be interpreted as the mean response at half the maximum resource density. How much the inflection points deviate from this mean response can be controlled by the parameter δ_{RED} (general symbol for $\delta_{NUT,rsa}$, $\delta_{NUT,amc}$, and $\delta_{WAT,rsa}$). If δ_{RED} is zero, there is no difference in the growth reduction between the species. If δ_{RED} larger than zero, species with higher trait values are less affected by nutrient or water stress:

$$x_{0,RED,txys} = \frac{1}{\beta_{RED}} \cdot \left(-\delta_{RED} \cdot \left(trait_{txys} - \left(\frac{1}{\delta_{RED}} \cdot \log\left(\frac{1 - \alpha_{RED,05}}{\alpha_{RED,05}}\right) + \phi_{trait}\right)\right)\right) + 0.5 \tag{14}$$

$$RED_{txys} = \begin{cases} 0 & \text{if } R_{txy} = 0 \\ 1/(1 + \exp(-\beta_{RED} \cdot (R_{txy} - x_{0,RED,txys}))) & \text{if } 0 < R_{txy} < 1 \\ 1 & \text{if } R_{txy} >= 1 \end{cases} \tag{15}$$

https://doi.org/10.5194/egusphere-2024-3798
Preprint. Discussion started: 17 December 2024

2.1.4 Species-specific nutrient stress

Plant growth may be reduced when soil nutrient availability is low and plants are poorly adapted. We consider arbuscular mycorrhizal colonisation rate (Marschner and Dell, 1994; George et al., 1995; Van Der Heijden et al., 2015) and root surface area per total biomass (Barber and Silberbush, 1984) as traits that help plants to take up nutrients and reduce nutrient stress. Here we only consider too little nutrients as nutrient stress. The growth reducer NUT_{txys} [−] is composed out of the maximum out of two nutrient stress factors that are linked to the arbuscular mycorrhizal colonization rate $N_{amc,txys}$ [−] and the root surface area per total biomass $N_{rsa,txys}$ [−]:

$$NUT_{txys} = \max(NUT_{amc,txys}, NUT_{rsa,txys}) \tag{16}$$

The maximum of the two nutrient stress factors is used, because plants can either invest in a high root surface area per total biomass or in a high arbuscular mycorrhizal colonization rate. Plants with a higher root surface area per total biomass follow the strategy of taking up nutrients themselves, while plants with a high arbuscular mycorrhizal colonisation rate follow the strategy of outsourcing nutrient uptake to arbuscular mycorrhizal fungi in the context of the root collaboration gradient (Bergmann et al., 2020). Since growth is reduced by how well plants follow their best strategy, the maximum of the two reduction factors is used to calculate the reduction in growth due to soil nutrients.

For the calculation of the growth reducers for nutrients stress based on the arbuscular mycorrhizal colonisation rate $NUT_{amc,txys}$ [−] we use the parameters ϕ_{TAMC} [−], $\beta_{NUT,amc}$ [−], $\alpha_{NUT,amc,05}$ [−], $\delta_{NUT,amc}$ [−] and for nutrients stress based on the root surface area per total biomass $NUT_{rsa,txys}$ [−] we use ϕ_{TRSA} [$\mathrm{m}^2 \cdot \mathrm{g}^{-1}$], $\beta_{NUT,rsa}$ [−], $\alpha_{NUT,rsa,05}$ [−], and $\delta_{NUT,rsa}$ [$\mathrm{g} \cdot \mathrm{m}^{-2}$]. Moreover, we still need trait values and the plant available nutrients (to replace $trait_s$ and R_{txy} in Eqs. 14-15).

For the traits that influence the nutrient growth reducer, we consider that plants with high below-ground biomass per total biomass are less affected by low nutrient levels because they have relatively more root tissue to supply nutrients to the above-ground biomass. It has been shown that the root-to-shoot ratio increases in many crops under nitrogen-poor conditions (Lopez et al., 2023). Therefore, we calculate the root surface area per total biomass $TRSA_{txys}$ [$\mathrm{m}^2 \cdot \mathrm{g}^{-1}$] and the arbuscular mycorrhizal colonisation rate per total biomass $TAMC_{txys}$ [−] from the fixed traits root surface area per below-ground biomass rsa_s and arbuscular mycorrhizal colonisation rate per root tissue amc_s with the dynamic proportion of the below-ground biomass $B_{B,txys}$ per total biomass B_{txys}:

$$TAMC_{txys} = \frac{B_{B,txys}}{B_{txys}} \cdot amc_s \tag{17}$$

$$TRSA_{txys} = \frac{B_{B,txys}}{B_{txys}} \cdot rsa_s \tag{18}$$

where the below-ground biomass is cancelled out. $TAMC_{txys}$ and $TRSA_txys$ are used to replace $trait$ in Equation 14 for the calculation of $NUT_{amc,txys}$ and $NUT_{rsa,txys}$.

The nutrients available to plants depend on the total nitrogen of a site and the density effect, which accounts for stronger competition for nutrients if many plant species have a high biomass. More technically, the total nitrogen N_{xy} [$\mathrm{g} \cdot \mathrm{kg}^{-1}$] is scaled between zero and one by the parameter $\alpha_{NUT,Nmax}$ [$\mathrm{g} \cdot \mathrm{kg}^{-1}$] and is multiplied by the nutrient adjustment factor

https://doi.org/10.5194/egusphere-2024-3798
Preprint. Discussion started: 17 December 2024

$NUT_{adj,txys}$ $[-]$, which accounts for the biomass density, to get the plant available nutrients $N_{p,txys}$ $[-]$:

$$N_{p,txys} = \frac{N_{xy}}{\alpha_{NUT,Nmax}} \cdot NUT_{adj,txys} \tag{19}$$

The plant available nutrients $N_{p,txys}$ are used in Equation 15 for the resource R_{txy} to calculate the growth reducers of $NUT_{amc,txys}$ and $NUT_{rsa,txys}$. $N_{p,txys}$ can be greater than one, if the total biomass is low, then growth is not reduced (see Eq. 15). In contrast to the plant available water (Eq. 26), the plant available nutrients are species-specific.

Plants are most strongly affected by below-ground competition if conspecifics and plants with similar traits have a high biomass and share the below-ground resources. This is summarized with the nutrient adjustment factor $NUT_{adj,txys}$ $[-]$ that takes into account the biomass and the trait similarity between all species:

$$NUT_{adj,txys} = \alpha_{NUT,maxadj} \cdot \exp\left(\log\left(\frac{1}{\alpha_{NUT,maxadj}}\right) \cdot \sum_{i=1}^{S} TS_{s,i} \cdot B_{txyi} \cdot \frac{1}{\alpha_{NUT,TSB}}\right) \tag{20}$$

with the trait similarity $TS_{s,i}$ $[-]$ between species s and i, the biomass of species i B_{txyi} $[\mathrm{kg} \cdot \mathrm{ha}^{-1}]$ and the parameters $\alpha_{NUT,TSB}$ $[\mathrm{kg} \cdot \mathrm{ha}^{-1}]$ and $\alpha_{NUT,maxadj}$ $[-]$. A high nutrient adjustment factor $NUT_{adj,txys}$ is favourable for a species because the factor is multiplied by the site nutrients (Eq. 19), which means that the species has to share the resources with fewer competitors. More specifically, a high $NUT_{adj,txys}$ of a species indicates that either the total biomass is low or the plant has traits that are very different from the traits of the abundant plant species. The parameter $\alpha_{NUT,TSB}$ is a reference value for the sum of the product of trait similarity and biomass of all species. If the sum of the product of trait similarity and biomass of all species is equal to $\alpha_{NUT,TSB}$, the nutrient adjustment factor is one. The parameter $\alpha_{NUT,maxadj}$ (≥ 1) controls the maximum of the nutrient adjustment factor. The parameter can be greater than one to allow the plant available nutrients to be increased when the total biomass is low.

The trait similarity is derived by calculating the dissimilarity of the root surface area per above-ground biomass rsa_s $[\mathrm{m}^2 \cdot \mathrm{g}^{-1}]$ and the arbuscular mycorrhizal colonization rate amc_s $[-]$ between all species and converting it to a similarity index. These two traits are chosen to calculate the trait dissimilarity index, because both traits encompass unique plant strategies for the acquisition of nutrients and water (Bergmann et al., 2020). The trait dissimilarity $TD_{s,i}$ $[-]$ between species s and species i is calculated with the euclidean distance between the normalized traits of the species:

$$AMC_{\mathrm{norm},s} = \frac{amc_s - \mathrm{mean}(\mathbf{amc})}{\mathrm{sd}(\mathbf{amc})} \tag{21}$$

$$RSA_{\mathrm{norm},s} = \frac{rsa_s - \mathrm{mean}(\mathbf{rsa})}{\mathrm{sd}(\mathbf{rsa})} \tag{22}$$

$$TD_{s,i} = \sqrt{\left(RSA_{\mathrm{norm},s} - RSA_{\mathrm{norm},i}\right)^2 + \left(AMC_{\mathrm{norm},s} - AMC_{\mathrm{norm},i}\right)^2} \tag{23}$$

https://doi.org/10.5194/egusphere-2024-3798
Preprint. Discussion started: 17 December 2024

This gives the dissimilarity matrix $\mathbf{TD}$ $[-]$, which is transformed and rescaled to a trait similarity matrix $\mathbf{TS}$ $[-]$:

$$\mathbf{TS} = 1 - \frac{\mathbf{TD}}{\max(\mathbf{TD})} \tag{24}$$

$$\mathbf{TS} = \begin{bmatrix} 1 & TS_{1,2} & \dots & TS_{1,S} \\ TS_{2,1} & 1 & & \\ \vdots & & \ddots & \\ TS_{S,1} & & & 1 \end{bmatrix} \tag{25}$$

2.1.5 Species-specific water stress

Plant growth may be reduced if soil water is low and the plants are poorly adapted. We consider the root surface area per total biomass $TRSA_{txys}$ $[\mathrm{m}^2 \cdot \mathrm{g}^{-1}]$ (see Eq. 18) as the trait that influences how strong plants are exposed to the water stress at a certain soil water level. Here, we only consider too little water leading to water stress conditions, not too much water. We use the same equations for the water stress reducer WAT_{txys} $[-]$ as for the nutrient reducer (see Eqs. 14-15) with the parameters ϕ_{TRSA} $[\mathrm{m}^2 \cdot \mathrm{g}^{-1}]$, $\beta_{WAT,rsa}$ $[-]$, $\alpha_{WAT,rsa,05}$ $[-]$, and $\delta_{WAT,rsa}$ $[\mathrm{g} \cdot \mathrm{m}^{-2}]$. The same explanation for the parameters applies as for the nutrient reducer.

The plant available water is the rescaled soil water content (to replace R in Eq. 15): The soil water content W_{txy} $[\mathrm{mm}]$ is scaled by the water holding capacity WHC_{xy} $[\mathrm{mm}]$ (Eq. 52) and the permanent wilting point PWP_{xy} $[\mathrm{mm}]$ (Eq. 53) to scale water availability between 0 (soil water content at or below the permanent wilting point) and 1 (soil water content at or above the water holding capacity). The plant available water $W_{p,txy}$ $[-]$ is defined as:

$$W_{p,txy} = \frac{W_{txy} - PWP_{xy}}{WHC_{xy} - PWP_{xy}} \tag{26}$$

2.1.6 Species-specific maintenance costs for roots and mycorrhizae

Maintaining a fine root structure and symbiosis with mycorrhizal fungi costs energy. These costs include respiration (Caldwell, 1979), the production of metabolites for nutrient uptake (Canarini et al., 2019), and the supply of photosynthetic products to the mycorrhizal fungi (Konvalinková et al., 2017). Similarly to Taubert et al. (2012), who consider the costs of maintaining a symbiosis with nitrogen-fixing rhizobia, we include a cost term for root surface area per total biomass $ROOT_{rsa,txys}$ $[-]$ and the mycorrhizal colonisation rate per total biomass $ROOT_{amc,txys}$ $[-]$. This means that part of the potential growth cannot be used to produce new biomass:

$$ROOT_{txys} = ROOT_{rsa,txys} \cdot ROOT_{amc,txys} \tag{27}$$

where $ROOT_{txys}$ $[-]$ is the root investment factor that lowers the actual growth in (Eq. 5).

$$ROOT_{rsa,txys} = 1 - \kappa_{ROOT,rsa} + \kappa_{ROOT,rsa} \cdot \exp\left(\frac{\log(0.5)}{\phi_{TRSA} \cdot TRSA_{txys}}\right) \tag{28}$$

$$ROOT_{amc,txys} = 1 - \kappa_{ROOT,amc} + \kappa_{ROOT,amc} \cdot \exp\left(\frac{\log(0.5)}{\phi_{TAMC} \cdot TAMC_{txys}}\right) \tag{29}$$

https://doi.org/10.5194/egusphere-2024-3798
Preprint. Discussion started: 17 December 2024

where $TRSA_{txys}$ is the root surface area per total biomass [$\mathrm{m}^2 \cdot \mathrm{g}^{-1}$] (see Eq. 18) and $TAMC_{txys}$ is the arbuscular mycorrhizal colonisation rate per total biomass [$-$] (see Eq. 17). The parameters $\kappa_{ROOT,rsa}$ [$-$] and $\kappa_{ROOT,amc}$ [$-$] define the maximum possible growth reduction from zero to one, where zero means no growth reduction at all. The parameters ϕ_{TRSA} [$\mathrm{m}^2 \cdot \mathrm{g}^{-1}$] and ϕ_{TAMC} [$-$] define the trait values of $TRSA_{txys}$ and $TAMC_{txys}$ at which the growth reducer is half in between 1 (no growth reduction) and the maximal growth reduction that is defined by $\kappa_{ROOT,rsa}$ and $\kappa_{ROOT,amc}$. Note that the same values for ϕ_{TRSA} and ϕ_{TAMC} are also used for water and nutrient stress reducers.

2.1.7 Community environmental and seasonal factors

The growth is adjusted for environmental and seasonal factors ENV_{txy} that apply in the same way to all species (Eq. 5). For simplicity, we do not consider the effect of specific-specific plant traits on the following functions:

$$ENV_{txy} = RAD_{txy} \cdot TEMP_{txy} \cdot SEA_{txy} \tag{30}$$

with the radiation RAD_{txy} [$-$] (Eq. 31), temperature $TEMP_{txy}$ [$-$] (Eq. 32), and seasonal SEA_{txy} [$-$] (Eq. 33) growth adjustment factors.

Plant growth increases with photosynthetically active radiation (as formulated in Eq. 6), but excess radiation can lead to oxidative damage and photoinhibition (Long et al., 1994). We have therefore included the equation and parametrisation from Schapendonk et al. (1998) that reduces the growth due to excess radiation. The radiation adjustment factor RAD_{txy} [$-$] is calculated as follows:

$$RAD_{txy} = \min\left(1, 1 - \gamma_{RAD,1}\left(PAR_{txy} - \gamma_{RAD,2}\right)\right) \tag{31}$$

with the photosynthetic active radiation PAR_{txy} [$\mathrm{MJ} \cdot \mathrm{ha}^{-1}$] and the parameters $\gamma_{RAD,1}$ [$\mathrm{MJ}^{-1} \cdot \mathrm{ha}$] and $\gamma_{RAD,2}$ [$\mathrm{MJ} \cdot \mathrm{ha}^{-1}$]. A linear decrease of radiation use efficiency with a steepness of $\gamma_{RAD,1}$ is assumed if the photosynthetic active radiation is above $\gamma_{RAD,2}$.

Temperature is one of the fundamental environmental factors that influence plant growth (Went, 1953). Thus, a temperature adjustment factor $TEMP_{txy}$ [$-$] is included in the model. The temperature adjustment factor is based on the equation by Schapendonk et al. (1998) that was adjusted by Jouven et al. (2006):

$$TEMP_{txy} = \begin{cases} 0 & \text{if } T_{txy} < \omega_{TEMP,T_1} \\ \frac{T_{txy} - \omega_{TEMP,T_1}}{\omega_{TEMP,T_2} - \omega_{TEMP,T_1}} & \text{if } \omega_{TEMP,T_1} < T_{txy} < \omega_{TEMP,T_2} \\ 1 & \text{if } \omega_{TEMP,T_2} < T_{txy} < \omega_{TEMP,T_3} \\ \frac{\omega_{TEMP,T_4} - T_{txy}}{\omega_{TEMP,T_4} - \omega_{TEMP,T_3}} & \text{if } \omega_{TEMP,T_3} < T_{txy} < \omega_{TEMP,T_4} \\ 0 & \text{if } T_{txy} > \omega_{TEMP,T_4} \end{cases} \tag{32}$$

with the minimum temperature requirement for growth ω_{TEMP,T_1} [°C], the optimum temperature for growth between ω_{TEMP,T_2} [°C] and ω_{TEMP,T_3} [°C] and the maximum temperature for growth ω_{TEMP,T_4} [°C]. The temperature adjustment factor in-

https://doi.org/10.5194/egusphere-2024-3798
Preprint. Discussion started: 17 December 2024

creases linearly from zero to one between ω_{TEMP,T_1} and ω_{TEMP,T_2}, stays at one between ω_{TEMP,T_2} and ω_{TEMP,T_3}, decreases linearly from one to zero between ω_{TEMP,T_3} and ω_{TEMP,T_4} and stays at zero above ω_{TEMP,T_4}.

A seasonal factor accounts for growth patterns that would not be expected from an analysis of daily abiotic conditions alone. Plants usually grow more strongly in spring than in autumn, even if the radiation and temperature values are similar. Therefore, in addition to the influence of radiation (Eqs. 6, 31) and temperature (Eq. 32) a seasonality factor is added. Jouven et al. (2006) build the following empirical step functions for the seasonal factor SEA_{txy} [−] based on the yearly accumulated degree days ST_{txy} [°C] and the parameters $\zeta_{SEA\min}$ [−], $\zeta_{SEA\max}$ [−], ζ_{SEA,ST_1} [°C], and ζ_{SEA,ST_2} [°C]:

$$SEA_{txy} = \begin{cases} \zeta_{SEA\min} & \text{if } ST_{txy} < 200\,^{\circ}\text{C} \\ \zeta_{SEA\min} + (\zeta_{SEA\max} - \zeta_{SEA\min}) \cdot \frac{ST_{txy} - 200\,^{\circ}\text{C}}{\zeta_{SEA,ST_1} - 400\,^{\circ}\text{C}} & \text{if } 200\,^{\circ}\text{C} < ST_{txy} < \zeta_{SEA,ST_1} - 200\,^{\circ}\text{C} \\ \zeta_{SEA\max} & \text{if } \zeta_{SEA,ST_1} - 200\,^{\circ}\text{C} < ST_{txy} < \zeta_{SEA,ST_1} - 100\,^{\circ}\text{C} \\ \zeta_{SEA\min} + (\zeta_{SEA\min} - \zeta_{SEA\max}) \cdot \frac{ST_{txy} - \zeta_{SEA,ST_2}}{\zeta_{SEA,ST_2} - \zeta_{SEA,ST_1} - 100\,^{\circ}\text{C}} & \text{if } \zeta_{SEA,ST_1} - 100\,^{\circ}\text{C} < ST_{txy} < \zeta_{SEA,ST_2} \\ \zeta_{SEA\min} & \text{if } ST_{txy} > \zeta_{SEA,ST_2} \end{cases} \tag{33}$$

$$ST_{txy} = \sum_{i=t \bmod 365}^{t} \max(0\,^{\circ}\text{C}, T_{ixy}) \tag{34}$$

The seasonality factor starts to increases from $\zeta_{SEA\min}$ to $\zeta_{SEA\max}$ with a yearly accumulated temperature of above 200 °C and reaches the maximum at $\zeta_{SEA,ST_1} - 200$ °C. From $\zeta_{SEA,ST_1} - 100$ °C to ζ_{SEA,ST_2} of the yearly accumulated the temperature the seasonality factor decreases from $\zeta_{SEA\max}$ to $\zeta_{SEA\min}$.

2.1.8 Species-specific senescence

Removal of plant biomass occurs through senescence and through management. The biomass removed by senescence S_{txys} [$\text{kg} \cdot \text{ha}^{-1}$] depends on the basic senescence rate α_{SEN} [month^{-1}], a seasonality factor SEN_{txy} [−], an effect of specific leaf area of the species sla_s [$\text{m}^2 \cdot \text{g}^{-1}$], and the biomass of the species B_{txys} [$\text{kg} \cdot \text{ha}^{-1}$]:

$$S_{txys} = \left(1 - (1 - \alpha_{SEN})^{1/30.44}\right) \cdot SEN_{txy} \cdot \left(\frac{sla_s}{\phi_{sla}}\right)^{\beta_{SEN,sla}} \cdot B_{txys} \tag{35}$$

While the basic senescence rate and seasonality factor are consistent across the plant community, the contribution of specific leaf area and biomass to the senescence rate varies between species. To facilitate interpretation, we have chosen to use the basic senescence rate per month α_{SEN}. Consequently, α_{SEN} has been converted to a senescence rate per day, assuming a monthly duration of 30.44 days. The influence of specific leaf area on senescence is controlled by two parameters: ϕ_{sla} [$\text{m}^2 \cdot \text{g}^{-1}$] and $\beta_{SEN,sla}$ [−]. $\beta_{SEN,sla}$ controls how much the senescence rate differs between species. If $\beta_{SEN,sla}$ is zero, there is no difference, and if $\beta_{SEN,sla}$ is large, there is a large difference in senescence rate between species. ϕ_{sla} is used as a reference for the specific leaf area values: if $sla_s < \phi_{sla}$ the senescence rate is less than α_{SEN}, if $sla_s = \phi_{sla}$ the senescence rate is equal

https://doi.org/10.5194/egusphere-2024-3798
Preprint. Discussion started: 17 December 2024

to α_{SEN} and if $sla_s > \phi_{sla}$ the senescence rate is greater than α_{SEN}. We included the effect of specific leaf on senescence rate because plant species with high specific leaf area are at the fast end of the leaf economic spectrum. This means that they tend to be highly photosynthetically efficient, modelled here with a higher leaf area index per biomass, but have a short leaf lifespan and therefore a high senescence rate (Wright et al., 2004).

A seasonality factor is used to account for the higher senescence in autumn. Depending on the cumulative temperate since the beginning of the current year ST_{txy} [°C] (Eq. 34) the seasonality factor increases from one [−] to a maximum $\psi_{SEN\,\max}$ [−]:

$$SEN_{txy} = \begin{cases} 1 & \text{if } ST_{txy} < \psi_{SEN,ST_1} \\ 1 + (\psi_{SEN\,\max} - 1)\frac{ST_{txy} - \psi_{SEN,ST_1}}{\psi_{SEN,ST_2} - \psi_{SEN,ST_1}} & \text{if } \psi_{SEN,ST_1} < ST_{txy} < \psi_{SEN,ST_2} \\ \psi_{SEN\,\max} & \text{if } ST_{txy} > \psi_{SEN,ST_2} \end{cases}, \tag{36}$$

where ψ_{SEN,ST_1} [°C] and ψ_{SEN,ST_2} [°C] are the temperature thresholds at which the seasonality factor starts to increase and reaches its maximum, respectively. The equation and the parameter values are based on Moulin et al. (2021) which is turn based on Jouven et al. (2006).

2.1.9 Management

Biomass losses M_{txys} [$\mathrm{kg \cdot ha^{-1}}$] due to management are caused by mowing MOW_{txys} [$\mathrm{kg \cdot ha^{-1}}$] (Eq. 38) and grazing GRZ_{txys} [$\mathrm{kg \cdot ha^{-1}}$] (Eq. 39) :

$$M_{txys} = MOW_{txys} + GRZ_{txys} \tag{37}$$

The biomass removed by mowing MOW_{txys} [$\mathrm{kg \cdot ha^{-1}}$] depends on the cutting height of the mowing machine and the height of the plant species. The proportion of above-ground plant biomass removed by mowing is defined by calculating the fraction of the plant height H_{txys} [m] above the cutting height CUT_{txy} [m] (see Table B1):

$$MOW_{txys} = \frac{\max(H_{txys} - CUT_{txy}, 0)}{H_{txys}} \cdot B_{A,txys}, \tag{38}$$

thereby assuming a uniform distribution of the biomass along the height of the plant.

The amount of biomass of one species that is fed by grazers depends on the livestock density, the palatability of the plant species that is linked to the leaf nitrogen content and the height of the plants. The grazing function GRZ_{txys} [$\mathrm{kg \cdot ha^{-1}}$] is divided into two parts: the first part defines the total grazed biomass and the second part distributes the grazed biomass among the plant species:

$$GRZ_{txys} = \frac{\kappa_{GRZ} \cdot LD_{txy} \cdot (B_{F,txy})^2}{(\kappa_{GRZ} \cdot LD_{txy} \cdot \eta_{GRZ})^2 + (B_{F,txy})^2} \cdot \frac{LNC_{GRZ,txys} \cdot H_{GRZ,txys} \cdot B_{F,txys}}{\sum_{i=1}^{S} LNC_{GRZ,txyi} \cdot H_{GRZ,txyi} \cdot B_{F,txyi}} \tag{39}$$

The variables and parameters are explained in the following two paragraphs.

For the total grazed biomass, we assume that grazers can only feed on plant biomass that is above a certain height $\epsilon_{GRZ,\min H}$ [m] (usually set to 0.05 m), because it has been shown that the intake rate of cattle decreases strongly with low sward height

https://doi.org/10.5194/egusphere-2024-3798
Preprint. Discussion started: 17 December 2024

(Hirata et al., 2010; Silva et al., 2018; Kunrath et al., 2020; Boval and Sauvant, 2021). Therefore, we calculate the above-ground biomass that can be fed by grazers $B_{F,txys}$ [$\mathrm{kg \cdot ha^{-1}}$] with the proportion of the above-ground biomass that is above the height $\epsilon_{GRZ,\min H}$:

$$B_{F,txys} = \max\left(1 - \frac{\epsilon_{GRZ,\min H}}{H_{txys}}, 0\right) \cdot B_{A,txys} \tag{40}$$

$$B_{F,txy} = \sum_{s=1}^{S} B_{F,txys} \tag{41}$$

where $B_{F,txy}$ [$\mathrm{kg \cdot ha^{-1}}$] is the total above-ground biomass that can be consumed by grazers. Furthermore, we assumed that if the overall reachable above-ground biomass is very low, the farmers will decide to provide additional fodder resulting in less grazed biomass. We do not include the fodder supply as an input in the model, but rather calculate it based on the above-ground biomass that is available to grazers. To incorporate this, we use a function that works similarly to a Holling type III response curve. The consumption of the grazers is determined by the product of the livestock density LD_{txy} [$\mathrm{LU \cdot ha^{-1}}$] (see Table B1) and the consumption per livestock and day κ_{GRZ} [$\mathrm{kg \cdot ha^{-1}}$]. We assume that the fodder supply equals half of the consumption of the grazers if the reachable above-ground biomass is equal to $LD_{txy} \cdot \kappa_{GRZ} \cdot \eta_{GRZ}$. By incorporating the livestock density in the term, we assume that the farmers will start earlier to supply additional fodder if the livestock density is high. The parameter η_{GRZ} [$-$] is a scaling parameter in the term. For example, if η_{GRZ} equals two, the total grazed biomass is reduced to half of the consumption at a reachable above-ground biomass that equals two times the consumption of the grazers.

The distribution of grazed biomass among plant species depends on their leaf nitrogen content, height, and the biomass accessible to grazers. The leaf nitrogent content factor $LNC_{GRZ,txys}$ [$-$] is based on the trait leaf nitrogen content per leaf mass lnc_s [$\mathrm{mg \cdot g^{-1}}$] relative to the community-weighted mean leaf nitrogen content per leaf mass $LNC_{cwm,txy}$ [$\mathrm{mg \cdot g^{-1}}$]

$$LNC_{GRZ,txys} = \left(\frac{lnc_s}{LNC_{cwm,txy}}\right)^{\beta_{GRZ,lnc}} \tag{42}$$

$$LNC_{cwm,txy} = \sum_{s=1}^{S} \frac{B_{F,txys}}{B_{F,txy}} \cdot lnc_s \tag{43}$$

with $\beta_{GRZ,lnc}$ [$-$] acting as a scaling exponent that defines how strongly the $LNC_{GRZ,txys}$ values deviate from one. This parameter thus controls the strength of the grazer's preference for plant species with high leaf nitrogen content. Empirical studies have demonstrated that cattle prefer plant species with high leaf nitrogen content (Pauler et al., 2020; Atkinson et al., 2024) and a high carbon to nitrogen ratio in leaves is associated with a grazing avoidance strategy (Archibald et al., 2019). Furthermore, we include a height factor because grazers feed more on plants that are tall and easily reachable (Hodgson et al., 1994). The height factor $H_{GRZ,txys}$ follows a similar equation as the leaf nitrogen factor, utilizing plant species H_{txys} in place of leaf nitrogen content relative to the community-weighted mean height $H_{cwm,txy}$ [m] and scaled by the exponent $\beta_{GRZ,H}$ [$-$]. In summary, the distribution of grazed biomass among plant species is driven by the biomass of the plant species, but can be altered by their relative leaf nitrogen content and height.

https://doi.org/10.5194/egusphere-2024-3798
Preprint. Discussion started: 17 December 2024

2.2 Plant height dynamics

Plant height H_{txys} increases due to growth but decreases with mowing and grazing. The height can increase until the plant reaches the maximum height $maxheight_s$ [m]. The growth rate is the ratio of above-ground biomass growth $A_{txys} \cdot G_{act,txys}$ (Eq. 3) to above-ground biomass $B_{A,txys}$. We consider the proportion of mown MOW_{txys} (Eq. 38) or grazed biomass GRZ_{txys} (Eq. 39) on the above-ground biomass as the proportion of height lost, assuming an even distribution of biomass along the height of the plant. Since leaves can die along the stem without reducing height, we assume that senescence has no effect on plant height:

$$H_{t+1xys} = H_{txys} \cdot \left(1 + \frac{A_{txys} \cdot G_{act,txys}}{B_{A,txys}} - \frac{MOW_{txys}}{B_{A,txys}} - \frac{GRZ_{txys}}{B_{A,txys}}\right) \tag{44}$$

2.3 Soil water dynamics

The change in the soil water content is influenced by multiple factors, including precipitation, evaporation, transpiration, and drainage and surface run-off. The equations follow Moulin et al. (2021) that are based on Schapendonk et al. (1998). The change in the soil water content W_{txy} [mm] is described by

$$W_{t+1xy} = W_{txy} + P_{txy} - AET_{txy} - R_{txy} \tag{45}$$

where P_{txy} is the precipitation [mm], AET_{txy} is the actual evapotranspiration [mm], and R_{txy} is the surface run-off and drainage of water from the soil [mm].

How strongly the soil surface is covered by vegetation influence whether more evaporation or transpiration occurs. This is modelled by the total leaf area index $LAI_{tot,txy}$ (Eqs. 9,10). If the soil is barely covered with vegetation, evaporation is higher than transpiration. Conversely, if the soil is well covered with vegetation, transpiration is higher than evaporation. Water can continue to evaporate from the soil as long as it contains water. Therefore, the potential evapotranspiration PET_{txy} [mm], which is a forcing function influencing both evaporation and transpiration (see Table B1), is multiplied by the fraction between the soil water content W_{txy} and the water holding capacity WHC_{xy} [mm] (Eq. 52) to obtain the evaporation E_{txy}:

$$E_{txy} = \frac{W_{txy}}{WHC_{xy}} \cdot PET_{txy} \cdot \left[1 - \min\left(1, \frac{LAI_{tot,txy}}{3}\right)\right] \tag{46}$$

On the other hand, plants can only transpire water that is available to them, so transpiration can only deplete the soil water content to the permanent wilting point. Therefore, the soil water content is rescaled by the permanent wilting point PWP_{xy} [mm] (Eq. 53) and the water holding capacity WHC_{xy} [mm] (Eq. 52) to a factor between zero and one that influences the amount of transpiration TR_{txy}:

$$TR_{txy} = \max\left(0, \frac{W_{txy} - PWP_{xy}}{WHC_{xy} - PWP_{xy}}\right) \cdot PET_{txy} \cdot \min\left(1, \frac{LAI_{tot,txy}}{3}\right) \tag{47}$$

Additionally, in contrast to Moulin et al. (2021), the transpiration depends here on a factor of the community-weighted mean specific leaf area SLA_{txy} [$m^2 \cdot g^{-1}$]. It was shown that species reduce the specific leaf area under drought stress (Wright et al.,

https://doi.org/10.5194/egusphere-2024-3798
Preprint. Discussion started: 17 December 2024

1993; Liu and Stützel, 2004) most likely to reduce transpiration. Therefore, it is here assumed that thinner leaves transpire more water. This relationship is modelled by the parameter $\alpha_{TR,sla}$ $[\mathrm{m}^2 \cdot \mathrm{g}^{-1}]$ that is the community-weighted mean specific leaf area where the factor equals one and $\beta_{TR,sla}$ $[-]$ that simulates how strongly the factor deviates from one if the community-weighted mean specific leaf area is below or above $\alpha_{TR,sla}$.

The actual evapotranspiration AET_{txy} [mm] is the sum of the evaporation E_{txy} [mm] and the transpiration TR_{txy} [mm] but cannot exceed the soil water content W_{txy} [mm]:

$$AET_{txy} = \min\left(W_{txy}, E_{txy} + TR_{txy}\right) \tag{48}$$

and any excess water above the water holding capacity WHC_{xy} [mm] (Eq. 52) is removed by surface run-off and drainage R_{txy} [mm]:

$$R_{txy} = \max\left(0\,\mathrm{mm}, W_{txy} + P_{txy} - AET_{txy} - WHC_{xy}\right) \tag{49}$$

Water holding capacity and permanent wilting point are derived from soil properties. Gupta and Larson (1979) show how the fraction of soil that can be filled with water F_{xy} can be related to particle size distribution, organic matter content and bulk density for different matrix potentials. This fraction was calculated for a matrix potential of -0.07 bar for the water holding capacity ($F_{WHC,xy}$) and for a matrix potential of -15 bar for the permanent wilting point ($F_{PWP,xy}$). The respective fraction was multiplied by the rooting depth to derive the water holding capacity and the permanent wilting point for the part of the soil that plants can reach with their roots:

$$\begin{aligned} F_{WHC,xy} = {} & \beta_{SND,WHC} \cdot SND_{xy} + \beta_{SLT,WHC} \cdot SLT_{xy} + \beta_{CLY,WHC} \cdot CLY_{xy} + \\ & \beta_{OM,WHC} \cdot OM_{xy} + \beta_{BLK,WHC} \cdot BLK_{xy} \end{aligned} \tag{50}$$

$$\begin{aligned} F_{PWP,xy} = {} & \beta_{SND,PWP} \cdot SND_{xy} + \beta_{SLT,PWP} \cdot SLT_{xy} + \beta_{CLY,PWP} \cdot CLY_{xy} + \\ & \beta_{OM,PWP} \cdot OM_{xy} + \beta_{BLK,PWP} \cdot BLK_{xy} \end{aligned} \tag{51}$$

$$WHC_{xy} = F_{WHC,xy} \cdot RD_{xy} \tag{52}$$

$$PWP_{xy} = F_{PWP,xy} \cdot RD_{xy} \tag{53}$$

3 Technical details of the GrasslandTraitSim.jl model

The model is implemented as a Julia package and can be used with the Julia programming language (Bezanson et al., 2017). It can be used on all major operating systems (Linux, MacOS, Windows). The model can be run on computers with low hardware requirements, as a 10-year simulation for one patch typically runs in less than half a second. A graphical user interface allows you to manually change parameter values and see the influence of each parameter on the simulation results (explained in more detail in the online documentation, see data accessibility statement). The model can be run on headless systems, but then the graphical user interface is not available. Throughout the model, units are used directly in the programming code using Unitful.jl, making the model easier to understand and debug. The outputs of the model have labelled axes using DimensionalData.jl,

https://doi.org/10.5194/egusphere-2024-3798
Preprint. Discussion started: 17 December 2024

making it easy to know which is the space, time or species axis. The package has extensive online documentation with all the equations, tutorials on how to set up the input data and how to analyse the output (see data accessibility statement). For each equation there are interactive plots to visualise the relationship between the variables and the influence of the parameters. Flowcharts are also available online to give a quick overview of the sub-processes. The model version described here can be installed in Julia using `import Pkg; Pkg.add("GrasslandTraitSim", version = "0.3.0")`. Later, the latest version can be installed using the same command without the version argument. The model is open source licenced under the GNU GPLv3 and contributions and collaboration are welcome. The development of the model is hosted at https://github.com/felixnoessler/GrasslandTraitSim.jl and new versions will be published in the General Julia package registry.

https://doi.org/10.5194/egusphere-2024-3798
Preprint. Discussion started: 17 December 2024

4 Calibration and validation of the model

For the calibration of the GrasslandTraitSim.jl model we used data from the Biodiversity Exploratories project (Fischer et al., 2010) from temperate grasslands of the Hainich-Dün region which is a hilly region in Central Germany. These include 50 permanent grassland sites with different intensities of grazing, mowing, and fertilization (Blüthgen et al., 2012). From these 50 sites, we selected those that were used as meadows or a mixture of pasture and meadow and excluded those that were used as pasture only, resulting in 28 sites. We decided to exclude the pasture sites because farmers often decided to provide supplementary feeding on these sites and the information on supplementary feeding is not detailed enough to be included in the simulation model. Most of these sites have a luvisol soil, with an average air temperature ~~temperature~~ of 9 °C, and a yearly precipitation sum of 700 mm.

We compiled input data for the model from different sources. Management data was used directly from the Biodiversity Exploratories project (timing and intensity of grazing and timing and height of mowing events, Vogt et al., 2024). We simplified the grazing input by including only one long grazing period instead of several short grazing periods as reported for some sites. We did this because the grazing information for some sites was not detailed enough. This simplification did not change the livestock density per hectare per year. Potential evapotranspiration was used from the AMBAV, an agro-meteorological model that outputs "potential evaporation over grass" from the nearby Mühlhausen weather station (DWD Climate Data Center, 2019) and is the same for all sites. Air temperature and precipitation were obtained for each site from the Biodiversity Exploraties project (Wöllauer et al., 2023). Photosynthetic activate radiation (PAR) was download with a three hours resolution from Wang (2021), the daily sum of PAR was obtained by calculating the integral of a quadratic regression to the PAR values. It was not possible to create site-specific PAR inputs due to the coarse resolution of the PAR data. Soil texture (Schöning et al., 2021c), rooting depth (Herold et al., 2021), bulk density (Schöning et al., 2021d) and organic matter content (Schöning et al., 2021b) were used from soil sampling campaigns of the Biodiversity Exploratories project. The total nitrogen concentration was aggregated from four years to get a mean overall total nitrogen concentration (Schöning et al., 2021b, e, a; Schöning, 2023). The trait data was compiled from species that are present in grasslands of the Biodiversity Exploratories project. Leaf area and leaf dry weight was sampled from individuals from sites of the Exploratories (Prati et al., 2021) to calculate the specific leaf area. The root surface area per below-ground biomass, arbuscular mycorrhizal colonisation rate and above-ground biomass per total biomass were obtained from individuals that were grown in a greenhouse experiment on sand (Bergmann and Rillig, 2022). The maximum height was obtained from Jäger et al. (2017) and the leaf nitrogen per leaf mass from the TRY database (Kattge et al. 2020, mainly from Gubsch et al. 2010; Pakeman et al. 2008; Schroeder-Georgi et al. 2016). We decided to set leaf biomass per plant biomass to 80 % of aboveground biomass per plant biomass for all species, as values for the trait leaf biomass per plant biomass were not available for many species. For 70 species we had values for all the traits. We used these 70 species as input for the simulation. During initialisation, the initial biomass of 5000 $\mathrm{kg \cdot ha^{-1}}$ was evenly distributed across all species and divided into above-ground and below-ground biomass according to the trait above-ground biomass per total biomass. The initial soil water content was set to 180 mm.

https://doi.org/10.5194/egusphere-2024-3798
Preprint. Discussion started: 17 December 2024

For the calibration and validation data we used the cut above-ground biomass and community-weighted mean traits. The biomass was cut once per year on every site at 4 cm height (Hinderling et al., 2024). The community-weighted mean traits were calculated based on the relative cover share of each plant species to the total cover. Each year, the cover of plant species was estimated on an area of 16 m^2 (Hinderling and Keller, 2023). We had more trait data available for the calculation of community weighted mean traits, as we could include all species with values for the trait currently being calculated, even if these species had missing values for other traits. Whereas we used input data from 2006 to 2021, we only used calibration data from 2010 to 2021 to allow for an initialisation phase of the grassland model. We sorted the sites from north to south and used the 14 sites in the north for calibration and the 14 sites in the south for validation. We chose this approach to reduce the spatial dependence between the calibration and validation datasets and to avoid repeating the computationally intensive training of the parameters several times, as in random K-fold cross-validation.

We wanted to minimise the mean absolute error between modelled and observed total biomass and community-weighted mean traits. However, the traits and biomass have different units, so they are not directly comparable. We therefore used the multi-objective optimization algorithm NSGA-II (Deb et al., 2002), as implemented in de Dios and Mezura-Montes (2022), to obtain the Pareto optimal front. We used a population of 100 parameter sets. We then selected the best parameter set of the population using the TOPSIS method (Hwang and Yoon, 1981). We assigned half the weight to total biomass and the other half equally to the community-weighted mean traits, this ensures that the fit for the traits together and above-ground biomass are equally important. For simplicity, we only present solutions from the parameter set with the highest score and show the best 25 parameter sets in the supplement (see data accessibility statement).

We included 23 parameters in the optimisation, 28 parameters were fixed. fixed parameter values were mostly obtained from literature (see Table B2). Upper and lower bounds of the optimised parameters were set so that they make sense, e.g. leaves with a low nitrogen content per leaf mass should not be preferred by grazers. The ranges of fixed and optimized parameters can be seen in the supplement (see data accessibility statement). For the light competition, we used the method with the height layers and the parameter $\beta_{LIG,H}$ has no influence on the simulation.

The results of the validation sites with the best and worst fit for the cut biomass indicate that the calibration worked, but also show difficulties in achieving ~~good results~~ satisfactory performance given the high number of objectives and sites (Fig. 4, all other sites in the supplement, see data accessibility statement). For example, the total above-ground biomass for the site HEG04 is estimated too low indicating that site specific charact cs are not reflected enough. Site differences in the model exist by different inputs namely management, climate and soil properties.

https://doi.org/10.5194/egusphere-2024-3798
Preprint. Discussion started: 17 December 2024

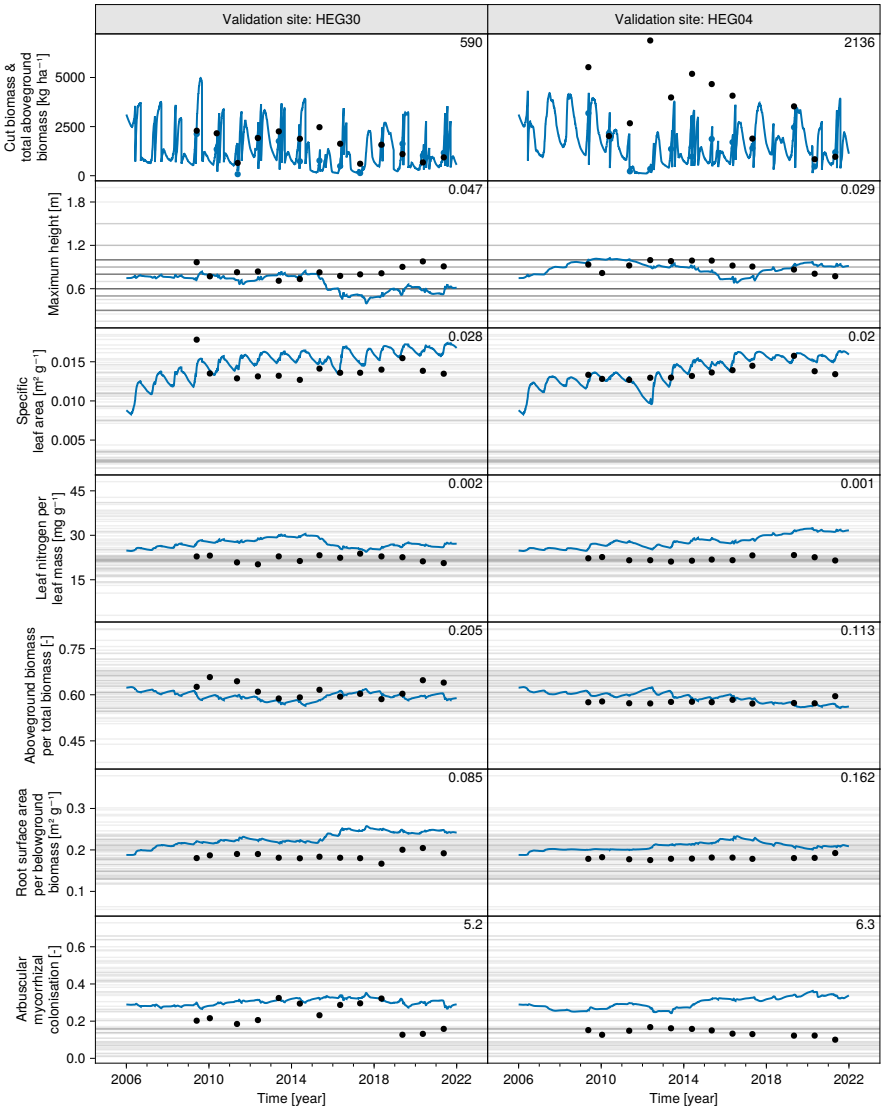

Figure 4. Results from validation sites with the best and the worst mean absolute error for the cut biomass. The mean absolute error is shown in the right upper corner of each subpanel. The horizontal grey lines depict the traits of the species. Black dots are observations (cut biomass) or derived from observations (community-weighted mean traits), the blue line is the simulation output. The blue dots in the first row show the simulated cut biomass, which is lower than the total above-ground biomass. Results for all calibration and validation sites are available in the supplementary material (see data accessibility statement)

https://doi.org/10.5194/egusphere-2024-3798
Preprint. Discussion started: 17 December 2024

5 Illustrative simulation experiments

In order to illustrate the capabilities of the GrasslandTraitSim.jl model, we present a simple scenario analysis. We want to explore the influence of land use intensity on community composition and plant functional diversity. As in the calibration and validation, we used the same input data from the 28 Hainich sites of the Biodiversity Exploratories project and the same initialisation with the same 70 species, initialising each species with a total biomass of $5000/70\ \mathrm{kg \cdot ha^{-1}}$ and a soil water content in the rooting zone of $150\ \mathrm{mm}$, but changed the land use input. We constructed two simulation experiments with either mowing only or grazing only. The number of mowing events was varied from one to five and the grazing intensity from May to August between a livestock density of 0.5 and 4 $\mathrm{ha \cdot d^{-1}}$ for each of the sites. Outside the grazing period from May to August, we set the grazing intensity always to zero. We then calculated from the second half of the simulation, from 01.01.2014 to 31.12.2021 (removing spin-up period from 2006 to 2013), for each site the mean overall total above- and below-ground biomass, the mean annual grazed and mown biomass, average species height (height weighted by the biomass proportion of the species), functional dispersion and functional evenness (Fig. 5). We decided to not include functional richness here because we would have to set an arbitrary function threshold. Moreover, we calculated community-weighted mean traits (Fig. 6) and show the relative abundance change of the species for all scenarios (Fig. B1 and for all other sites in the supplement,see data accessibility statement).

The community composition changes with increasing land use intensity and land use type. As an illustrative simulation experiment, we do not interpret the results in much detail here. As two prominent traits we describe first the changes in height and second the changes in specific leaf area of the plants species with increasing land use intensity. First, the average height of the plants decreases with stronger land uses (see Fig. 5) as mowing and grazing both reduces the height of plants. In the same way, the community-weighted mean maximum height is reduced under high land use intensities (Fig. 6). Species with high maximum height are replaced by species with lower maximum height at higher land use intensities (Fig. B1) because they are less affected by mowing and grazing in the model. Second, the community-weighted mean specific leaf area increases with increasing land use intensity (Fig. 6). Again, species with a low specific leaf area are replaced by species with a higher specific leaf area in high land use scenarios (Fig. B1). This lends support to the quick return strategy of plants with a high specific leaf area outlined by Wright et al. (2004). The simulated community-weighted mean specific leaf areas and maximum plant heights in response to grazing agree with the results of Díaz et al. (2001), who showed that plant species with higher abundance on heavily grazed sites are small and have a high specific leaf area. Pauler et al. (2020) showed that cattle prefer to feed on tall species with a high specific leaf area, implying that species with a high specific leaf area are fed more but also have a higher regrowth rate. ~~Inline~~ In line with our results, mowing increase the specific leaf area within species and across communities (Bouchet et al., 2017; Zhang et al., 2023). In order to demonstrate the potential applications of the GrasslandTraitSim.jl model, we have included functional diversity indices. However, as we did not include functional diversity in the calibration, we hesitate to give much weight to the interpretation of the results. Still, we think that the GrasslandTraitSim.jl model can be used in further studies to analyse land use effects on plant community composition.

https://doi.org/10.5194/egusphere-2024-3798
Preprint. Discussion started: 17 December 2024

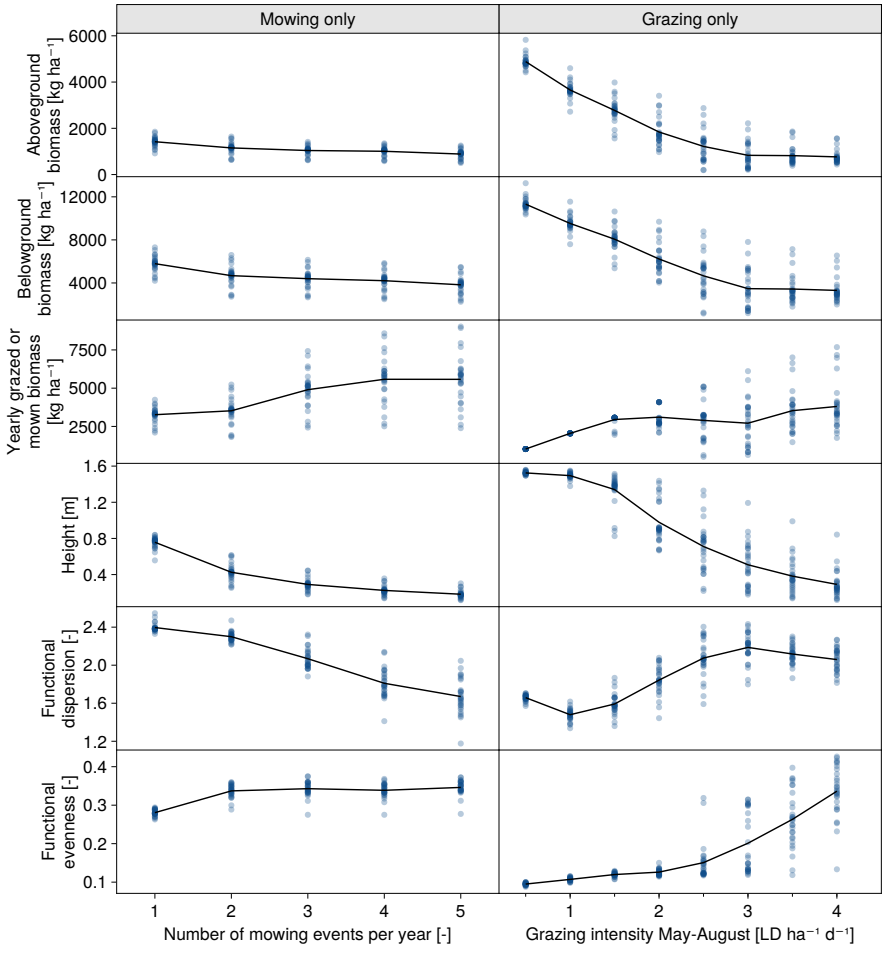

Figure 5. Changes in above-ground and below-ground biomass, yearly grazed and mown biomass, height and functional dispersion and evenness for 28 sites in response to different land use scenarios. In the left column, land use consists of mowing events only, whereas in the right column, grazing intensity was varied between scenarios. For each land use scenario, time series were simulated from all 28 sites and response variables were calculated based on the second half of the time series from 2014 to 2021. While the blue dots represent the results from the individual sites, the black line is the mean of all 28 sites.

https://doi.org/10.5194/egusphere-2024-3798
Preprint. Discussion started: 17 December 2024

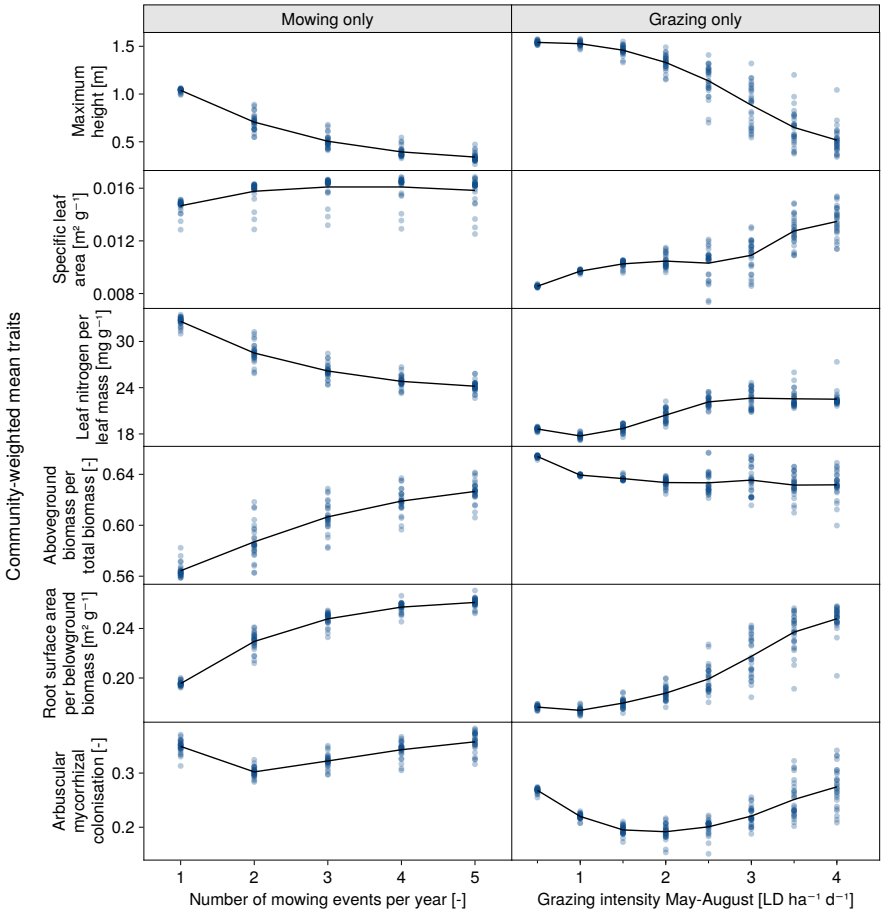

Figure 6. Changes in community-weighted mean traits in response to different land use scenarios. In the left column, land use consists of mowing events only, whereas in the right column, grazing intensity was varied between scenarios. For each land use scenario, time series were simulated from all 28 sites and the community-weighted mean traits were calculated based on the second half of the time series from 2014 to 2021. While the blue dots represent the community-weighted mean traits from the individual sites, the black line is the mean of all 28 sites.

https://doi.org/10.5194/egusphere-2024-3798
Preprint. Discussion started: 17 December 2024

6 Conclusions and outlook

We presented the process-based model GrasslandTraitSim.jl. The model can be used to simulate the effects of land use and climate change on the plant functional composition and on the provision of ecosystem services such as biomass production. In addition, the model is suitable to analyse the role of plant diversity in the provision of ecosystem services. We have extended the approach of Chalmandrier et al. (2021) to link measurements of morphological plant traits with demographic and physiological species-specific processes. The model can simulate the biomass and height of many plant species over time using only morphological traits as species-specific inputs.

However, the number of coexisting species (e.g. with biom 2 %) is still low, with three to five species accounting for most of the biomass in most scenario analyses. Future studies, could analyse the role of different coexistence mechanisms for species coexistence. In the current model implementation, grazing and mowing removes proportionally more biomass from species with a higher biomass (as these species tend to be taller), and we included a form of negative sity dependence in the nutrient competition. It was suggested that negative pla il feedbacks may play an important role in plant coexistence in grasslands (Bonanomi et al., 2005; Liu et al., 2022; Goossens et al., 2023). This could be taken into account by increasing the senescence rate with higher biomass, and could be coupled with the trait similarity approach that we have already used for nutrient competition. In biological terms, this would mean that plant pathogens prefer plant species with similar traits, and that pathogens spread more easily when plant species have high biomass. We believe that the GrasslandTraitSim.jl model is suitable for exploring species coexistence in response to land use and climate change can in future studies.

This article has a strong focus on model description. We are aware of some limitations, for example that a total biomass value per year may not be sufficient to calibrate a simulation model with a daily time step, and that we have not calibrated below-ground biomass, he and soil water content in the rooting zone. In order to further explore the range of applicability of the model, we plan to conduct a subsequent calibration study with multiple data sets.

This study can be seen as a step towards modelling highly diverse plant communities in grasslands. We hope that the documentation, tutorials and open source code will lead to collaborations and discussion on the topic.

https://doi.org/10.5194/egusphere-2024-3798
Preprint. Discussion started: 17 December 2024

Appendix A: Derivation of the species-specific water and nutrient growth reducers

The response curves (growth reducers) RED_{txys} for different nutrient and water availabilities, denoted as R_{txy}, are implemented via logistic equations with a minimum of zero (no growth is possible) and a maximum of one (no growth reduction). While the species-specific part of the response curves is implemented by different inflection points $x_{0,RED,txys}$, the slope β_{RED} is the same for all species:

$$RED_{txys} = \frac{1}{1+\exp\left(-\beta_{RED}\cdot\left(R_{txy}-x_{0,RED,txys}\right)\right)} \tag{A1}$$

We then used another logistic equation that relates the trait values to the inflection point of the response curve. We wanted to control how much the response curves should differ when the trait values differ from $x_{0,prep,s}$, this is implemented with the parameter δ_{RED}. The equation could be written as:

$$x_{0,RED,txys} = x_{0,RED,\min} + \frac{x_{0,RED,\max}-x_{0,RED,\min}}{1+\exp\left(-\delta_{RED}\cdot\left(trait_{txys}-x_{0,prep,s}\right)\right)} \tag{A2}$$

However, this equations and their parameter $x_{0,prep,s}$, $x_{0,RED,\min}$, and $x_{0,RED,\max}$ are hard to understand and to interpret, therefore we reformulated the equation. Instead of calculating the inflection point $x_{0,RED,txys}$ directly, we calculated the growth reduction at 0.5 of the maximal resource availability:

$$RED_{05,txys} = \frac{1}{1+\exp\left(-\delta_{RED}\cdot\left(trait_{txys}-x_{0,RED,05}\right)\right)} \tag{A3}$$

This has the advantage that we have natural boundaries $\in [0,1]$, because the growth reduction cannot be larger than one ($RED_{txys}=0$) or lower than zero ($RED_{txys}=1$). We introduce one parameter $\alpha_{RED,05}$ that is the growth reducer for the mean trait ϕ_{trait} at half of the maximal resource availability:

$$\alpha_{RED,05} = \frac{1}{1+\exp\left(-\delta_{RED}\cdot\left(\phi_{trait}-x_{0,R,05}\right)\right)} \tag{A4}$$

and rearranged the equation to:

$$x_{0,R,05} = \frac{1}{\delta_{RED}}\cdot\log\left(\frac{1-\alpha_{RED,05}}{\alpha_{RED,05}}\right)+\phi_{trait} \tag{A5}$$

This leads to an equation that we can use to calculate the growth reducer for all trait values at half of the maximal resource availability:

$$RED_{05,txys} = \frac{1}{1+\exp\left(-\delta_{RED}\cdot\left(trait_{txys}-\left(\frac{1}{\delta_{RED}}\cdot\log\left(\frac{1-\alpha_{RED,05}}{\alpha_{RED,05}}\right)+\phi_{trait}\right)\right)\right)} \tag{A6}$$

Now, we need again the full equation to calculate the growth reducer for any resource availability. We use the Equation A1 and solve for $x_{0,RED,txys}$ with $RED_{txys}=0.5$:

$$RED_{05,txys} = \frac{1}{1+\exp\left(-\beta_{RED}\cdot\left(0.5-x_{0,RED,txys}\right)\right)} \tag{A7}$$

https://doi.org/10.5194/egusphere-2024-3798
Preprint. Discussion started: 17 December 2024

to get the inflection point $x_{0,RED,txys}$:

$$x_{0,RED,txys} = \frac{1}{\beta_R} \cdot \log\left(\frac{1 - RED_{05,txys}}{RED_{05,txys}}\right) + 0.5 \tag{A8}$$

Thus, the full equation to calculate the growth reducer for any resource availability is:

$$RED_{txys} = \frac{1}{1 + \exp\left(-\beta_{RED} \cdot \left(R_{txy} - \left(\frac{1}{\beta_{RED}} \cdot \log\left(\frac{1-RED_{05,txys}}{RED_{05,txys}}\right) + 0.5\right)\right)\right)} \tag{A9}$$

and with everything combined and simplified:

$$RED_{txys} = \frac{1}{1 + \exp\left(-\beta_{RED} \cdot \left(R_{txy} - \left[\frac{1}{\beta_{RED}} \cdot \left(-\delta_{RED} \cdot \left(trait_{txys} - \left(\frac{1}{\delta_{RED}} \cdot \log\left(\frac{1-\alpha_{RED,05}}{\alpha_{RED,05}}\right) + \phi_{trait}\right)\right)\right) + 0.5\right]\right)\right)} \tag{A10}$$

Note the species-specific inflection point $x_{0,RED,txys}$ in square brackets.

https://doi.org/10.5194/egusphere-2024-3798
Preprint. Discussion started: 17 December 2024

Appendix B: Species response and use intensity

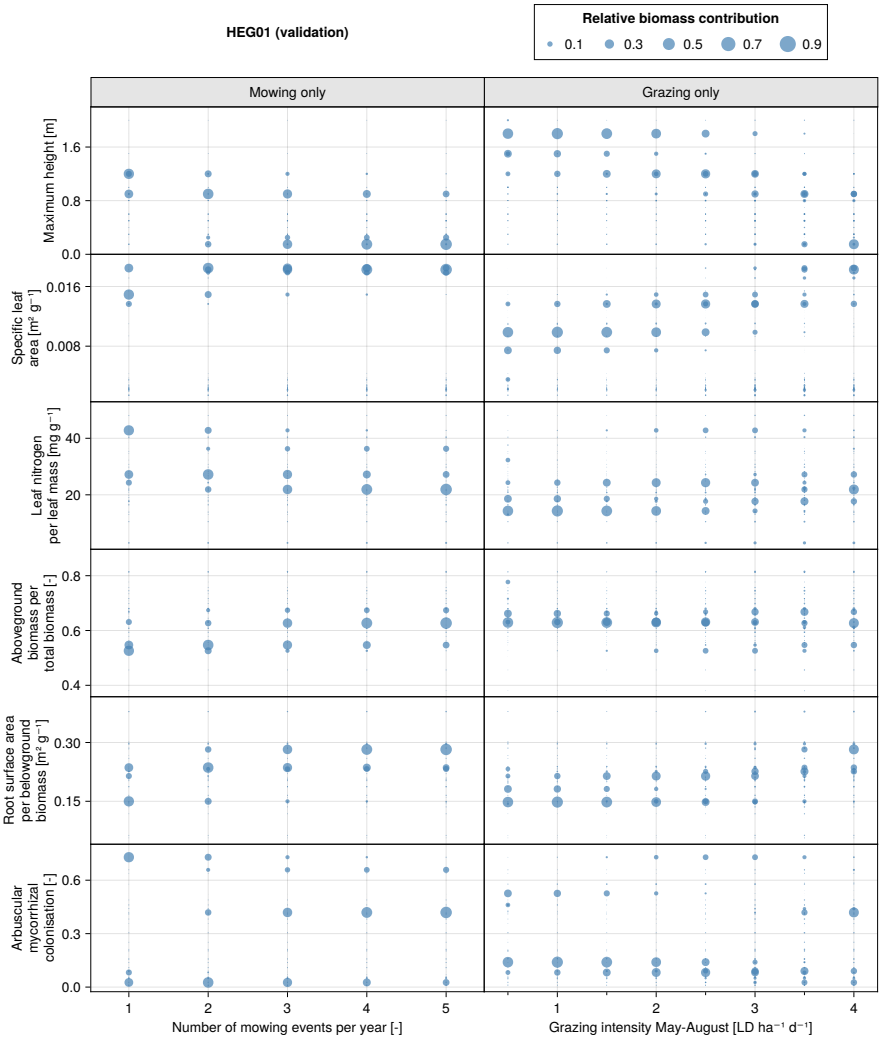

Figure B1. Change in relative abundance of plant species in response to different land use scenarios for the site HEG01. The traits of the species are fixed, only the abundance of the species can change. In the left column, land use consists of mowing events only, whereas in the right column, grazing intensity was varied between scenarios. For each land use scenario, time series were calculated and the second half of the time series, from 2014 to 2021, was used to calculate the average biomass share of total biomass for each species. Figures for all other sites can be found in the supplement (see data accessibility statement) and the summary over all sites can be seen in the main text in Fig. 6.

https://doi.org/10.5194/egusphere-2024-3798
Preprint. Discussion started: 17 December 2024

Table B1. Input variables of the model. The dimensions of the variables are given in the subscript of the symbols: t per day, x, y per patch, s per species. The patch dimensions for the climate, management and soil variables are optional.

Sym.	Variable	Unit
Climate		
PAR_{txy}	Photosynthetic active radiation	$\mathrm{MJ} \cdot \mathrm{ha}^{-1}$
T_{txy}	Mean air temperature	°C
P_{txy}	Precipitation	mm
PET_{txy}	Potential evapotranspiration	mm
Management		
CUT_{txy}	Cutting height for mowing	m or NaN
LD_{txy}	Livestock density	ha^{-1} or NaN
Soil		
SND_{xy}	Sand content (proportion $\in [0, 1]$)	–
SLT_{xy}	Silt content (proportion $\in [0, 1]$)	–
CLY_{xy}	Clay content (proportion $\in [0, 1]$)	–
OM_{xy}	Organic matter content (proportion $\in [0, 1]$)	–
BLK_{xy}	Bulk density	$\mathrm{g} \cdot \mathrm{cm}^{-3}$
RD_{xy}	Rooting depth of plants	mm
N_{xy}	Total nitrogen in the soil	$\mathrm{g} \cdot \mathrm{kg}^{-1}$
Morphological plant traits		
$maxheight_s$	Maximum plant height	m
sla_s	Specific leaf area	$\mathrm{m}^2 \cdot \mathrm{kg}^{-1}$
lnc_s	Leaf nitrogen content per leaf mass	$\mathrm{mg} \cdot \mathrm{g}^{-1}$
rsa_s	Root surface area per below-ground biomass	$\mathrm{m}^2 \cdot \mathrm{g}^{-1}$
amc_s	Arbuscular mycorrhizal colonization rate	–
abp_s	above-ground biomass per total biomass	–
lbp_s	Leaf biomass per total biomass	–

650

https://doi.org/10.5194/egusphere-2024-3798
Preprint. Discussion started: 17 December 2024

Table B2. Parameters of the model and the references for the parameter values.

Symbol	Parameter	Value	Unit	Reference
Reference traits				
ϕ_{TRSA}	Reference root surface area per total biomass, used in nutrient stress function and maintenance costs for roots function, set to mean of community: $\phi_{TRSA} = \text{mean}((1-\mathbf{abp})\cdot\mathbf{rsa})$	≈ 0.07	$\text{m}^2 \cdot \text{g}^{-1}$	-
ϕ_{TAMC}	Reference arbuscular mycorriza colonisation rate per total biomass, used in nutrient stress function and maintenance costs for mycorrhizae function, set to mean of community: $\phi_{TAMC} = \text{mean}((1-\mathbf{abp})\cdot\mathbf{amc})$	≈ 0.11	$-$	-
ϕ_{sla}	Reference specific leaf area, used in senescence function, set to mean of community: $\phi_{sla} = \text{mean}(\mathbf{sla})$	≈ 0.009	$\text{m}^2 \cdot \text{g}^{-1}$	-
Light interception and competition				
γ_{RUEmax}	Maximum radiation use efficiency	0.003	$\text{kg} \cdot \text{MJ}^{-1}$	Schapendonk et al. (1998)
$\gamma_{RUE,k}$	Light extinction coefficient	0.6	$-$	Schapendonk et al. (1998)
$\alpha_{RUE,cwmH}$	Reduction factor of radiation use efficiency at a height of 0.2 m $\in [0,1]$	calibrated	$-$	-
$\beta_{LIG,H}$	Exponent that coontrols how strongly taller plants intercept more light than smaller plants	calibrated	$-$	-
Water stress				
$\alpha_{WAT,rsa,05}$	Water stress growth reduction factor for species with mean trait: $TRSA = \phi_{TRSA}$, when the plant available water equals: $W_{p,txy} = 0.5$	calibrated	$-$	-
$\beta_{WAT,rsa}$	Slope of the logistic function that relates the plant available water to the water stress growth reduction factor	calibrated	$-$	-
$\delta_{WAT,rsa}$	Controls how strongly species differ in their water stress growth reduction from the mean response	calibrated	$\text{g} \cdot \text{m}^{-2}$	
Nutrient stress				
$\alpha_{NUT,Nmax}$	Maximum total soil nitrogen, on all the grassland sites of the Biodiversity Exploratories, the maximum total soil nitrogen is 30 $\text{g} \cdot \text{kg}^{-1}$	35	$\text{g} \cdot \text{kg}^{-1}$	-
$\alpha_{NUT,TSB}$	Reference value, if the sum of the product of trait similarity and biomass of all species equals: $\sum TS \cdot B < 1$, $\sum TS \cdot B = 1$, $\sum TS \cdot B > 1$ the nutrient adjustment factor $NUT_{adj,txys}$ is higher than one, one and lower than one, respectively	calibrated	$\text{kg} \cdot \text{ha}^{-1}$	-

https://doi.org/10.5194/egusphere-2024-3798
Preprint. Discussion started: 17 December 2024

$\alpha_{NUT,maxadj}$	Maximum of the nutrient adjustment factor, fixed for calibration	10	–	-
$\alpha_{NUT,amc,05}$	Nutrient stress based on arbuscular mycorriza colonisation growth reduction factor for species with mean trait: $TAMC = \phi_{TAMC}$, when the plant available nutrients equal: $N_{p,txys} = 0.5$	calibrated	–	-
$\alpha_{NUT,rsa,05}$	Nutrient stress based on root surface area growth reduction factor for species with mean trait: $TRSA = \phi_{TRSA}$, when the plant available nutrients equal: $N_{p,txys} = 0.5$	calibrated	–	-
$\beta_{NUT,amc}$	Slope of the logistic function that relates the plant available nutrients to the nutrient stress growth reduction factor based on arbuscular mycorriza colonisation	calibrated	–	-
$\beta_{NUT,rsa}$	Slope of the logistic function that relates the plant available nutrients to the nutrient stress growth reduction factor based on root surface area	calibrated	–	-
$\delta_{NUT,amc}$	Controls how strongly species differ in their nutrients stress growth reduction based on arbuscular mycorriza colonisation from the mean response	calibrated	–	
$\delta_{NUT,rsa}$	Controls how strongly species differ in their nutrient stress growth reduction based on root surface area from the mean response	calibrated	$\mathrm{g \cdot m^{-2}}$	
Maintenance costs for roots and mycorrhizae				
$\kappa_{ROOT,amc}$	Maximum growth reduction due to maintenance costs for mycorrhizae based on arbuscular mycorriza colonisation rate	calibrated	–	-
$\kappa_{ROOT,rsa}$	Maximum growth reduction due to maintenance costs for fine roots based on root surface area	calibrated	–	-
Environmental and seasonal growth adjustment				
$\gamma_{RAD,1}$	Controls the steepness of the linear decrease in radiation use efficiency for high PAR_{txy} values	$4.45 \cdot 10^{-6}$	$\mathrm{MJ^{-1}}$	Schapendonk et al. (1998)
$\gamma_{RAD,2}$	Threshold value of PAR_{txy} from which starts a linear decrease in radiation use efficiency	$5 \cdot 10^{4}$	$\mathrm{MJ \cdot ha^{-1}}$	Schapendonk et al. (1998)
ω_{TEMP,T_1}	Minimum temperature for growth	4	°C	Jouven et al. (2006)
ω_{TEMP,T_2}	Lower limit of optimum temperature for growth	10	°C	Schapendonk et al. (1998)
ω_{TEMP,T_3}	Upper limit of optimum temperature for growth	20	°C	Jouven et al. (2006)
ω_{TEMP,T_4}	Maximum temperature for growth	35	°C	Moulin et al. (2021)
ζ_{SEA,ST_1}	Threshold of the cumulative temperate since the beginning of the current year, the seasonality factor starts to decrease from $\zeta_{SEA\,\max}$ to $\zeta_{SEA\,\min}$ above $\zeta_{SEA,ST_1} - 100$	calibrated	°C	-

https://doi.org/10.5194/egusphere-2024-3798
Preprint. Discussion started: 17 December 2024

ζ_{SEA,ST_2}	Threshold of the cumulative temperate since the beginning of the current year, above which the seasonality factor is set to $\zeta_{SEA\,\min}$	calibrated	°C	-
$\zeta_{SEA\,\min}$	Minimum value of the seasonal growth effect	calibrated	–	-
$\zeta_{SEA\,\max}$	Maximum value of the seasonal growth effect	calibrated	–	-
Senescence				
α_{SEN}	Basic senescence rate	calibrated	month^{-1}	-
$\beta_{SEN,sla}$	Controls the influence of the specific leaf area on the senescence rate	calibrated	–	-
ψ_{SEN,ST_1}	Threshold of the cumulative temperate since the beginning of the current year above which the senescence begins to increase	calibrated	°C	-
ψ_{SEN,ST_2}	Threshold of the cumulative temp since the beginning of the current year above which the senescence reaches the maximum senescence rate $\psi_{SEN\,\max}$	3000	°C	Moulin et al. (2021)
$\psi_{SEN\,\max}$	Maximum senescence rate	calibrated	–	-
Management				
$\beta_{GRZ,lnc}$	Controls the influence of leaf nitrogen per leaf mass on grazer preference	calibrated	–	-
$\beta_{GRZ,H}$	Controls the influence of height on grazer preference	calibrated	–	-
η_{GRZ}	Scaling factor that controls at which biomass density additional feed is supplied by farmers, fixed for calibration	2	–	-
κ_{GRZ}	Consumption of dry biomass per livestock and day	22	$\mathrm{kg \cdot ha}^{-1}$	Gillet (2008)
$\epsilon_{GRZ,\min H}$	Minimum height that is reachable by grazers	0.05	m	cf. Hirata et al. (2010)
Water dynamics				
$\beta_{SND,WHC}$,	Slope parameter relating the sand, silt, clay, organic matter	0.5678,	–,	Gupta and Larson (1979)
$\beta_{SLT,WHC}$,	content and the bulk density to the soil water content at the	0.9228,	–,	
$\beta_{CLY,WHC}$,	water holding capacity	0.9135,	–,	
$\beta_{OM,WHC}$,		0.6103,	–,	
$\beta_{BLK,WHC}$		−0.2696	$\mathrm{cm}^3 \cdot \mathrm{g}^{-1}$	
$\beta_{SND,PWP}$,	Slope parameter relating the sand, silt, clay, organic matter	−0.0059,	–,	Gupta and Larson (1979)
$\beta_{SLT,PWP}$,	content and the bulk density to the soil water content at the	0.1142,	–,	
$\beta_{CLY,PWP}$,	permanent wilting point	0.5766,	–,	
$\beta_{OM,PWP}$,		0.2228,	–,	
$\beta_{BLK,PWP}$		0.02671	$\mathrm{cm}^3 \cdot \mathrm{g}^{-1}$	

https://doi.org/10.5194/egusphere-2024-3798
Preprint. Discussion started: 17 December 2024

Table B3. Overview of the model equations and their references. New means that the equations are newly composed for the grassland model and were not adopted from other grassland models.

Eq.	Topic	References
Main biomass dynamic		
1	main biomass dynamic	similar to Schapendonk et al. (1998); Moulin et al. (2021)
2	ratio between above-ground and below-ground biomass	new
3	change in above-ground biomass	new
4	change in below-ground biomass	new
5	actual growth	similar to Schapendonk et al. (1998); Moulin et al. (2021)
Light interception and competition		
6	potential growth	Eq. (1) of Lacasa et al. (2021), Monsi and Saeki (2005)
7	fraction of the radiation that is intercepted	for Beer–Lambert equation see Monsi and Saeki (2005); Lacasa et al. (2021), added the influence of the community height
8	community-weighted mean height	general equation
9	total leaf area index	general equation
10	leaf area index	Watson (1947)
11	simple method for light competition	for fraction of leaf area index see Moulin et al. (2021), added influence of height
12	light interception in vertical layers of the sward	similar to Taubert et al. (2012)
13	vertical layers method for light competition	similar to Taubert et al. (2012)
General form of the growth reducer for nutrient and water stress		
14	species-specific inflection point of logistic growth reduction function for nutrient and water stress	new
15	logistic growth reduction function for nutrient and water stress	new
Nutrient stress		
16	nutrient stress growth reduction factor	new
17	arbuscular mycorrhizal colonisation rate per total biomass	new
18	root surface area per total biomass	new
19	plant available nutrients	
20	nutrient adjustment factor based on biomass and trait similarity	new
21	normalized arbuscular mycorrhizal colonisation rate	general equation
22	normalized root surface area per below-ground biomass	general equation
23	trait dissimilarity index	new

https://doi.org/10.5194/egusphere-2024-3798
Preprint. Discussion started: 17 December 2024

24	trait similarity calculation	new
25	trait similarity as matrix	new
Water stress		
26	plant available water	Moulin et al. (2021)
Maintenance costs for roots and mycorrhizae		
27	costs for roots and mycorrhizae growth reduction factor	new
28	costs for fine roots reduction factor	new
29	costs for mycorrhizae growth reduction factor	new
Environmental and seasonal growth adjustment		
30	environmental and seasonal growth adjustment	Moulin et al. (2021)
31	growth reduction based on too high radiation	Schapendonk et al. (1998)
32	temperature growth reducer function	Schapendonk et al. (1998), Jouven et al. (2006), Moulin et al. (2021)
33	seasonal growth adjustment	Jouven et al. (2006), Moulin et al. (2021)
34	yearly accumulated temperature	Jouven et al. (2006), Moulin et al. (2021)
Senescence		
35	senescence rate	Moulin et al. (2021), added influence of specific leaf area
36	seasonality of senescence	Moulin et al. (2021)
Management		
37	biomass losses due to management	similar to Moulin et al. (2021)
38	mown biomass	influence of plant height to mowing tolerance similar to the λ in Moulin et al. (2021)
39	grazed biomass	partly based on Moulin et al. (2021); added influence of leaf nitrogen content and height on grazer preference
42	influence of leaf nitrogen per leaf mass on grazer preference	new
43	community-weighted mean leaf nitrogen content	general equation
Plant height dynamics		
44	change in the plant height	new
Water dynamic		
45	main soil water dynamic	Schapendonk et al. (1998), Moulin et al. (2021)
46	evaporation	Moulin et al. (2021)
47	transpiration	simplified/modified from Moulin et al. (2021)
48	actual evapotranspiration	Moulin et al. (2021)
49	water drainage and run-off	Moulin et al. (2021)

https://doi.org/10.5194/egusphere-2024-3798
Preprint. Discussion started: 17 December 2024

50	fraction of the soil that can be filled with water at the water holding capacity	Gupta and Larson (1979)
51	fraction of the soil that can be filled with water at the permanent wilting point	Gupta and Larson (1979)
52	water holding capacity in the rooting zone	Gupta and Larson (1979)
53	permanent wilting point in the rooting zone	Gupta and Larson (1979)

https://doi.org/10.5194/egusphere-2024-3798
Preprint. Discussion started: 17 December 2024

Code and data availability. The model code, scripts for calibration, and raw and processed data for the calibration and validation can be found on Zenodo with DOI: 10.5281/zenodo.14011849 (Nößler, 2024). This work is partly based on data of the Biodiversity Exploratories program (DFG Priority Program 1374). The datasets are publicly available in the Biodiversity Exploratories Information System (http://doi.org/10.17616/R32P9Q), with links to the specific datasets in the reference section, and are included in the Zenodo repository. The documentation with tutorials can be found online at https://felixnoessler.github.io/GrasslandTraitSim.jl/v0.3/. Details on methods and results of the calibration and of the simulation experiment for all sites can be seen online at https://felixnoessler.github.io/calibration_grasslandtraitsim_v1/. Especially relevant are the subsite on the ranges for optimized parameters (https://felixnoessler.github.io/calibration_grasslandtraitsim_v1/parameter_optimized.html), the calibration/validation results for all sites (https://felixnoessler.github.io/calibration_grasslandtraitsim_v1/calibration_results_sites.html), and the results of the scenario analysis for all sites (https://felixnoessler.github.io/calibration_grasslandtraitsim_v1/calibration_results_scenario.html).

Author contributions. Conceptualization: FN, FM, TM, and OB. Methodology: FN and TM. Software, Formal analysis, Visualization, and Writing – original draft: FN. Writing – review and editing: FN, BT, TM, FM, and OB. Supervision: FM, OB, BT, and TM.

Competing interests. The contact author has declared that none of the authors has any competing interests.

Acknowledgements. We would like to thank Florian Hartig for the discussion on calibration and Joana Bergmann for the discussion on below-ground plant traits. We would like to thank the HPC service of the FUB-IT, Freie Universität Berlin for the computing time provided (Bennett et al., 2020). We acknowledge support by the Open Access Publication Fund of Freie Universität Berlin. We thank the managers of the the Hainich-Exploratory Anna K. Franke and Robert Künast and all former managers for their work in maintaining the plot and project infrastructure; Victoria Grießmeier for giving support through the central office, Andreas Ostrowski for managing the central data base, and Markus Fischer, Eduard Linsenmair, Dominik Hessenmöller, Daniel Prati, Ingo Schöning, François Buscot, Ernst-Detlef Schulze, Wolfgang W. Weisser and the late Elisabeth Kalko for their role in setting up the Biodiversity Exploratories project. We thank the administration of the Hainich national park as well as all land owners for the excellent collaboration. The work has been (partly) funded by the DFG Priority Program 1374 "Biodiversity- Exploratories". Field work permits were issued by the responsible state environmental offices of Thüringen.

https://doi.org/10.5194/egusphere-2024-3798
Preprint. Discussion started: 17 December 2024

References

Adler, P. B., Seabloom, E. W., Borer, E. T., Hillebrand, H., Hautier, Y., Hector, A., Harpole, W. S., O'Halloran, L. R., Grace, J. B., Anderson, T. M., Bakker, J. D., Biederman, L. A., Brown, C. S., Buckley, Y. M., Calabrese, L. B., Chu, C.-J., Cleland, E. E., Collins, S. L., Cottingham, K. L., Crawley, M. J., Damschen, E. I., Davies, K. F., DeCrappeo, N. M., Fay, P. A., Firn, J., Frater, P., Gasarch, E. I., Gruner, D. S., Hagenah, N., Hille Ris Lambers, J., Humphries, H., Jin, V. L., Kay, A. D., Kirkman, K. P., Klein, J. A., Knops, J. M. H., La Pierre, K. J., Lambrinos, J. G., Li, W., MacDougall, A. S., McCulley, R. L., Melbourne, B. A., Mitchell, C. E., Moore, J. L., Morgan, J. W., Mortensen, B., Orrock, J. L., Prober, S. M., Pyke, D. A., Risch, A. C., Schuetz, M., Smith, M. D., Stevens, C. J., Sullivan, L. L., Wang, G., Wragg, P. D., Wright, J. P., and Yang, L. H.: Productivity Is a Poor Predictor of Plant Species Richness, Science, 333, 1750–1753, https://doi.org/10.1126/science.1204498, 2011.

Archibald, S., Hempson, G. P., and Lehmann, C.: A unified framework for plant life-history strategies shaped by fire and herbivory, New Phytologist, 224, 1490–1503, https://doi.org/10.1111/nph.15986, 2019.

Atkinson, J., Gallagher, R., Czyżewski, S., Kerr, M., Trepel, J., Buitenwerf, R., and Svenning, J.: Integrating functional traits into trophic rewilding science, Journal of Ecology, https://doi.org/10.1111/1365-2745.14307, 2024.

Barber, S. A. and Silberbush, M.: Plant Root Morphology and Nutrient Uptake, in: Roots, Nutrient and Water Influx, and Plant Growth, pp. 65–87, https://doi.org/10.2134/asaspecpub49.c4, 1984.

Bennett, L., Melchers, B., and Proppe, B.: Curta: A General-purpose High-Performance Computer at ZEDAT, Freie Universität Berlin, https://doi.org/10.17169/REFUBIUM-26754, 2020.

Bergmann, J. and Rillig, M.: Fine root and mycorrhizal traits of 82 grassland species measured in a greenhouse experiment on sand, 2018, https://www.bexis.uni-jena.de/ddm/data/Showdata/26546?version=2, dataset ID: 26546, 2022.

Bergmann, J., Weigelt, A., van der Plas, F., Laughlin, D. C., Kuyper, T. W., Guerrero-Ramirez, N., Valverde-Barrantes, O. J., Bruelheide, H., Freschet, G. T., Iversen, C. M., Kattge, J., McCormack, M. L., Meier, I. C., Rillig, M. C., Roumet, C., Semchenko, M., Sweeney, C. J., van Ruijven, J., York, L. M., and Mommer, L.: The fungal collaboration gradient dominates the root economics space in plants, Science Advances, 6, eaba3756, https://doi.org/10.1126/sciadv.aba3756, 2020.

Bezanson, J., Edelman, A., Karpinski, S., and Shah, V. B.: Julia: A fresh approach to numerical computing, SIAM Rev. Soc. Ind. Appl. Math., 59, 65–98, https://doi.org/10.1137/141000671, 2017.

Blüthgen, N., Dormann, C. F., Prati, D., Klaus, V. H., Kleinebecker, T., Hölzel, N., Alt, F., Boch, S., Gockel, S., Hemp, A., Müller, J., Nieschulze, J., Renner, S. C., Schöning, I., Schumacher, U., Socher, S. A., Wells, K., Birkhofer, K., Buscot, F., Oelmann, Y., Rothenwöhrer, C., Scherber, C., Tscharntke, T., Weiner, C. N., Fischer, M., Kalko, E. K. V., Linsenmair, K. E., Schulze, E.-D., and Weisser, W. W.: A quantitative index of land-use intensity in grasslands: Integrating mowing, grazing and fertilization, Basic and Applied Ecology, 13, 207–220, https://doi.org/10.1016/j.baae.2012.04.001, 2012.

Bonanomi, G., Giannino, F., Mazzoleni, S., and Setälä, H.: Negative Plant-Soil Feedback and Species Coexistence, Oikos, 111, 311–321, https://doi.org/10.1111/j.0030-1299.2005.13975.x, 2005.

Bouchet, D. C., Cheptou, P.-O., and Munoz, F.: Mowing influences community-level variation in resource-use strategies and flowering phenology along an ecological succession on Mediterranean road slopes, Applied Vegetation Science, 20, 376–387, https://doi.org/10.1111/avsc.12311, 2017.

Boval, M. and Sauvant, D.: Ingestive behaviour of grazing ruminants: Meta-analysis of the components linking bite mass to daily intake, Animal Feed Science and Technology, 278, 115 014, https://doi.org/10.1016/j.anifeedsci.2021.115014, 2021.

https://doi.org/10.5194/egusphere-2024-3798
Preprint. Discussion started: 17 December 2024

Caldwell, M. M.: Root Structure: The Considerable Cost of Belowground Function, in: Topics in Plant Population Biology, edited by Solbrig, O. T., Jain, S., Johnson, G. B., and Raven, P. H., pp. 408–427, Macmillan Education UK, London, ISBN 978-1-349-04627-0, https://doi.org/10.1007/978-1-349-04627-0_18, 1979.

Canarini, A., Kaiser, C., Merchant, A., Richter, A., and Wanek, W.: Root Exudation of Primary Metabolites: Mechanisms and Their Roles in Plant Responses to Environmental Stimuli, Frontiers in Plant Science, 10, https://doi.org/10.3389/fpls.2019.00157, 2019.

Chalmandrier, L., Hartig, F., Laughlin, D. C., Lischke, H., Pichler, M., Stouffer, D. B., and Pellissier, L.: Linking functional traits and demography to model species-rich communities, Nature Communications, 12, https://doi.org/10.1038/s41467-021-22630-1, 2021.

Chen, S., Wang, W., Xu, W., Wang, Y., Wan, H., Chen, D., Tang, Z., Tang, X., Zhou, G., Xie, Z., Zhou, D., Shangguan, Z., Huang, J., He, J.-S., Wang, Y., Sheng, J., Tang, L., Li, X., Dong, M., Wu, Y., Wang, Q., Wang, Z., Wu, J., Chapin, F. S., and Bai, Y.: Plant diversity enhances productivity and soil carbon storage, Proceedings of the National Academy of Sciences, 115, 4027–4032, https://doi.org/10.1073/pnas.1700298114, 2018.

Clark, J. S., Carpenter, S. R., Barber, M., Collins, S., Dobson, A., Foley, J. A., Lodge, D. M., Pascual, M., Pielke Jr, R., and Pizer, W.: Ecological forecasts: an emerging imperative, science, 293, 657–660, https://doi.org/10.1126/science.293.5530.657, 2001.

de Dios, J.-A. M. and Mezura-Montes, E.: Metaheuristics: A Julia Package for Single- and Multi-Objective Optimization, Journal of Open Source Software, 7, 4723, https://doi.org/10.21105/joss.04723, 2022.

Deb, K., Pratap, A., Agarwal, S., and Meyarivan, T.: A fast and elitist multiobjective genetic algorithm: NSGA-II, IEEE Transactions on Evolutionary Computation, 6, 182–197, https://doi.org/10.1109/4235.996017, 2002.

Dee, L. E., Ferraro, P. J., Severen, C. N., Kimmel, K. A., Borer, E. T., Byrnes, J. E. K., Clark, A. T., Hautier, Y., Hector, A., Raynaud, X., Reich, P. B., Wright, A. J., Arnillas, C. A., Davies, K. F., MacDougall, A., Mori, A. S., Smith, M. D., Adler, P. B., Bakker, J. D., Brauman, K. A., Cowles, J., Komatsu, K., Knops, J. M. H., McCulley, R. L., Moore, J. L., Morgan, J. W., Ohlert, T., Power, S. A., Sullivan, L. L., Stevens, C., and Loreau, M.: Clarifying the effect of biodiversity on productivity in natural ecosystems with longitudinal data and methods for causal inference, Nature Communications, 14, 2607, https://doi.org/10.1038/s41467-023-37194-5, 2023.

DWD Climate Data Center: Calculated daily values for different characteristic elements of soil and crops., https://opendata.dwd.de/climate_environment/CDC/derived_germany/soil/daily/historical/, version v19.3. Accessed on 09.03.2023, 2019.

Díaz, S., Noy-Meir, I., and Cabido, M.: Can grazing response of herbaceous plants be predicted from simple vegetative traits?, Journal of Applied Ecology, 38, 497–508, https://doi.org/10.1046/j.1365-2664.2001.00635.x, 2001.

European Environment Agency, Kühn, E., Pettersson, L., Strien, A., Õunap, E., Warren, M., Settele, J., Švitra, G., Botham, M., Regan, E., Prokofev, I., Swaay, C., Stefanescu, C., Heliölä, J., Popov, S., Roth, T., Leopold, P., Verovnik, R., Fontaine, B., Musche, M., Julliard, R., Collins, S., Goloshchapova, S., Öberg, S., Cornish, N., Brereton, T., Titeux, N., Harpke, A., and Roy, D.: The European grassland butterfly indicator – 1990–2011, Publications Office of the European Union, https://doi.org/10.2800/89760, 2013.

Eurostat: Main farm land use by NUTS 2 regions, https://doi.org/10.2908/ef_lus_main, 2020.

Fischer, M., Bossdorf, O., Gockel, S., Hänsel, F., Hemp, A., Hessenmöller, D., Korte, G., Nieschulze, J., Pfeiffer, S., Prati, D., Renner, S., Schöning, I., Schumacher, U., Wells, K., Buscot, F., Kalko, E. K. V., Linsenmair, K. E., Schulze, E.-D., and Weisser, W. W.: Implementing large-scale and long-term functional biodiversity research: The Biodiversity Exploratories, Basic and Applied Ecology, 11, 473–485, https://doi.org/10.1016/j.baae.2010.07.009, 2010.

Fort, H.: On predicting species yields in multispecies communities: Quantifying the accuracy of the linear Lotka-Volterra generalized model, Ecological Modelling, 387, 154–162, https://doi.org/10.1016/j.ecolmodel.2018.09.009, 2018.

https://doi.org/10.5194/egusphere-2024-3798
Preprint. Discussion started: 17 December 2024

Geijzendorffer, I. R., van der Werf, W., Bianchi, F. J. J. A., and Schulte, R. P. O.: Sustained dynamic transience in a Lotka–Volterra competition model system for grassland species, Ecological Modelling, 222, 2817–2824, https://doi.org/10.1016/j.ecolmodel.2011.05.029, 2011.

George, E., Marschner, H., and Jakobsen, I.: Role of Arbuscular Mycorrhizal Fungi in Uptake of Phosphorus and Nitrogen From Soil, Critical Reviews in Biotechnology, 15, 257–270, https://doi.org/10.3109/07388559509147412, 1995.

Gillet, F.: Modelling vegetation dynamics in heterogeneous pasture-woodland landscapes, Ecological Modelling, 217, 1–18, https://doi.org/10.1016/j.ecolmodel.2008.05.013, 2008.

Goossens, E. P., Minden, V., Van Poucke, F., and Olde Venterink, H.: Negative plant-soil feedbacks disproportionally affect dominant plants, facilitating coexistence in plant communities, npj Biodiversity, 2, 27, https://doi.org/10.1038/s44185-023-00032-4, 2023.

Gossner, M. M., Lewinsohn, T. M., Kahl, T., Grassein, F., Boch, S., Prati, D., Birkhofer, K., Renner, S. C., Sikorski, J., Wubet, T., Arndt, H., Baumgartner, V., Blaser, S., Blüthgen, N., Börschig, C., Buscot, F., Diekötter, T., Jorge, L. R., Jung, K., Keyel, A. C., Klein, A.-M., Klemmer, S., Krauss, J., Lange, M., Müller, J., Overmann, J., Pašalić, E., Penone, C., Perović, D. J., Purschke, O., Schall, P., Socher, S. A., Sonnemann, I., Tschapka, M., Tscharntke, T., Türke, M., Venter, P. C., Weiner, C. N., Werner, M., Wolters, V., Wurst, S., Westphal, C., Fischer, M., Weisser, W. W., and Allan, E.: Land-use intensification causes multitrophic homogenization of grassland communities, Nature, 540, 266–269, https://doi.org/10.1038/nature20575, 2016.

Griffin-Nolan, R. J., Blumenthal, D. M., Collins, S. L., Farkas, T. E., Hoffman, A. M., Mueller, K. E., Ocheltree, T. W., Smith, M. D., Whitney, K. D., and Knapp, A. K.: Shifts in plant functional composition following long-term drought in grasslands, Journal of Ecology, 107, 2133–2148, https://doi.org/10.1111/1365-2745.13252, 2019.

Gubsch, M., Buchmann, N., Schmid, B., Schulze, E.-D., Lipowsky, A., and Roscher, C.: Differential effects of plant diversity on functional trait variation of grass species, Annals of Botany, 107, 157–169, https://doi.org/10.1093/aob/mcq220, 2010.

Gupta, S. C. and Larson, W. E.: Estimating soil water retention characteristics from particle size distribution, organic matter percent, and bulk density, Water Resources Research, 15, 1633–1635, https://doi.org/10.1029/WR015i006p01633, 1979.

Heger, T.: Light availability experienced in the field affects ability of following generations to respond to shading in an annual grassland plant, Journal of Ecology, 104, 1432–1440, https://doi.org/10.1111/1365-2745.12607, 2016.

Hejcman, M., Hejcmanová, P., Pavlů, V., and Beneš, J.: Origin and history of grasslands in Central Europe – a review, Grass and Forage Science, 68, 345–363, https://doi.org/10.1111/gfs.12066, 2013.

Herold, N., Schöning, I., and Schrumpf, M.: Soil Survey 2008 Subplot Description, https://www.bexis.uni-jena.de/ddm/data/Showdata/4761?version=3, dataset ID: 4761, 2021.

Hilpold, A., Seeber, J., Fontana, V., Niedrist, G., Rief, A., Steinwandter, M., Tasser, E., and Tappeiner, U.: Decline of rare and specialist species across multiple taxonomic groups after grassland intensification and abandonment, Biodiversity and Conservation, 27, 3729–3744, https://doi.org/10.1007/s10531-018-1623-x, 2018.

Hinderling, J. and Keller, S.: Vegetation records for grassland EPs, 2008 - 2022, https://www.bexis.uni-jena.de/ddm/data/Showdata/31389?version=7, dataset ID: 31389, 2023.

Hinderling, J., Penone, C., Prati, D., Bolliger, R., Schäfer, D., Boch, S., and Schmitt, B.: Biomass data for grassland EPs, 2009 - 2023, https://www.bexis.uni-jena.de/ddm/data/Showdata/31581?version=5, dataset ID: 31581, 2024.

Hirata, M., Kunieda, E., and Tobisa, M.: Short-term ingestive behaviour of cattle grazing tropical stoloniferous grasses with contrasting growth forms, The Journal of Agricultural Science, 148, 615–624, https://doi.org/10.1017/S0021859610000353, 2010.

https://doi.org/10.5194/egusphere-2024-3798
Preprint. Discussion started: 17 December 2024

Hodgson, J., Clark, D., and Mitchell, R.: Foraging Behavior in Grazing Animals and Its Impact on Plant Communities, in: Forage Quality, Evaluation, and Utilization, pp. 796–827, https://doi.org/10.2134/1994.foragequality.c19, 1994.

Hwang, C.-L. and Yoon, K.: Multiple Attribute Decision Making, Springer Berlin Heidelberg, https://doi.org/10.1007/978-3-642-48318-9, 1981.

Jeltsch, F., Moloney, K. A., Schurr, F. M., Köchy, M., and Schwager, M.: The state of plant population modelling in light of environmental change, Perspectives in Plant Ecology, Evolution and Systematics, 9, 171–189, https://doi.org/10.1016/j.ppees.2007.11.004, 2008.

Jouven, M., Carrère, P., and Baumont, R.: Model predicting dynamics of biomass, structure and digestibility of herbage in managed permanent pastures. 1. Model description, Grass and Forage Science, 61, 112–124, https://doi.org/10.1111/j.1365-2494.2006.00515.x, 2006.

Jäger, E. J., Müller, F., Ritz, C., Welk, E., and Wesche, K., eds.: Rothmaler - Exkursionsflora von Deutschland, Gefäßpflanzen: Atlasband, Springer Berlin Heidelberg, ISBN 9783662497104, https://doi.org/10.1007/978-3-662-49710-4, 2017.

Kattge, J., Bönisch, G., Díaz, S., Lavorel, S., Prentice, I. C., Leadley, P., Tautenhahn, S., Werner, G. D. A., et al.: TRY plant trait database – enhanced coverage and open access, Global Change Biology, 26, 119–188, https://doi.org/10.1111/gcb.14904, 2020.

Kipling, R. P., Virkajärvi, P., Breitsameter, L., Curnel, Y., De Swaef, T., Gustavsson, A.-M., Hennart, S., Höglind, M., Järvenranta, K., Minet, J., Nendel, C., Persson, T., Picon-Cochard, C., Rolinski, S., Sandars, D. L., Scollan, N. D., Sebek, L., Seddaiu, G., Topp, C. F. E., Twardy, S., Van Middelkoop, J., Wu, L., and Bellocchi, G.: Key challenges and priorities for modelling European grasslands under climate change, Science of The Total Environment, 566-567, 851–864, https://doi.org/10.1016/j.scitotenv.2016.05.144, 2016.

Konvalinková, T., Püschel, D., Řezáčová, V., Gryndlerová, H., and Jansa, J.: Carbon flow from plant to arbuscular mycorrhizal fungi is reduced under phosphorus fertilization, Plant and Soil, 419, 319–333, https://doi.org/10.1007/s11104-017-3350-6, 2017.

Kunrath, T. R., Nunes, P. A. d. A., de Souza Filho, W., Cadenazzi, M., Bremm, C., Martins, A. P., and Carvalho, P. C. d. F.: Sward height determines pasture production and animal performance in a long-term soybean-beef cattle integrated system, Agricultural Systems, 177, 102 716, https://doi.org/10.1016/j.agsy.2019.102716, 2020.

Lacasa, J., Hefley, T. J., Otegui, M. E., and Ciampitti, I. A.: A practical guide to estimating the light extinction coefficient with nonlinear models—a case study on maize, Plant Methods, 17, https://doi.org/10.1186/s13007-021-00753-2, 2021.

Liu, F. and Stützel, H.: Biomass partitioning, specific leaf area, and water use efficiency of vegetable amaranth (Amaranthus spp.) in response to drought stress, Scientia Horticulturae, 102, 15–27, https://doi.org/https://doi.org/10.1016/j.scienta.2003.11.014, 2004.

Liu, X., Parker, I. M., Gilbert, G. S., Lu, Y., Xiao, Y., Zhang, L., Huang, M., Cheng, Y., Zhang, Z., and Zhou, S.: Coexistence is stabilized by conspecific negative density dependence via fungal pathogens more than oomycete pathogens, Ecology, 103, https://doi.org/10.1002/ecy.3841, 2022.

Long, S. P., Humphries, S., and Falkowski, P. G.: Photoinhibition of Photosynthesis in Nature, Annual Review of Plant Physiology and Plant Molecular Biology, 45, 633–662, https://doi.org/10.1146/annurev.pp.45.060194.003221, 1994.

Lopez, G., Ahmadi, S. H., Amelung, W., Athmann, M., Ewert, F., Gaiser, T., Gocke, M. I., Kautz, T., Postma, J., Rachmilevitch, S., Schaaf, G., Schnepf, A., Stoschus, A., Watt, M., Yu, P., and Seidel, S. J.: Nutrient deficiency effects on root architecture and root-to-shoot ratio in arable crops, Frontiers in Plant Science, 13, https://doi.org/10.3389/fpls.2022.1067498, 2023.

Marschner, H. and Dell, B.: Nutrient uptake in mycorrhizal symbiosis, Plant and Soil, 159, 89–102, https://doi.org/10.1007/bf00000098, 1994.

May, F., Grimm, V., and Jeltsch, F.: Reversed effects of grazing on plant diversity: the role of below-ground competition and size symmetry, Oikos, 118, 1830–1843, https://doi.org/10.1111/j.1600-0706.2009.17724.x, 2009.

Monsi, M.: Uber den Lichtfaktor in den Pflanzengesellschaften und seine Bedeutung fur die Stoffproduktion, Jap. J. Bot., 14, 22–52, 1953.

https://doi.org/10.5194/egusphere-2024-3798
Preprint. Discussion started: 17 December 2024

Monsi, M. and Saeki, T.: On the Factor Light in Plant Communities and its Importance for Matter Production, Annals of Botany, 95, 549–567, https://doi.org/10.1093/aob/mci052, 2005.

Monteith, J. L.: Solar Radiation and Productivity in Tropical Ecosystems, Journal of Applied Ecology, 9, 747–766, https://doi.org/10.2307/2401901, 1972.

Moulin, T., Perasso, A., Calanca, P., and Gillet, F.: DynaGraM: A process-based model to simulate multi-species plant community dynamics in managed grasslands, Ecological Modelling, 439, 109 345, https://doi.org/10.1016/j.ecolmodel.2020.109345, 2021.

Movedi, E., Bellocchi, G., Argenti, G., Paleari, L., Vesely, F., Staglianò, N., Dibari, C., and Confalonieri, R.: Development of generic crop models for simulation of multi-species plant communities in mown grasslands, Ecological Modelling, 401, 111–128, https://doi.org/10.1016/j.ecolmodel.2019.03.001, 2019.

Nagy, S.: Grasslands as a bird habitat, in: Grasslands in Europe: Of High Nature Value, pp. 35–41, KNNV Publishing, ISBN 9789004278103, https://doi.org/10.1163/9789004278103_005, 2009.

Nößler, F.: Supplementary material: A trait-based model to describe plant community dynamics in managed grasslands (GrasslandTraitSim.jl v1.0.0), https://doi.org/10.5281/zenodo.14011849, 2024.

Pakeman, R. J., Garnier, E., Lavorel, S., Ansquer, P., Castro, H., Cruz, P., Doležal, J., Eriksson, O., Freitas, H., Golodets, C., Kigel, J., Kleyer, M., Lepš, J., Meier, T., Papadimitriou, M., Papanastasis, V. P., Quested, H., Quétier, F., Rusch, G., Sternberg, M., Theau, J.-P., Thébault, A., and Vile, D.: Impact of abundance weighting on the response of seed traits to climate and land use, Journal of Ecology, 96, 355–366, https://doi.org/10.1111/j.1365-2745.2007.01336.x, 2008.

Parton, W.: The CENTURY model, in: Evaluation of soil organic matter models: Using existing long-term datasets, pp. 283–291, Springer, https://doi.org/10.1007/978-3-642-61094-3_23, 1996.

Parton, W. J., Hartman, M., Ojima, D., and Schimel, D.: DAYCENT and its land surface submodel: description and testing, Global and Planetary Change, 19, 35–48, https://doi.org/10.1016/S0921-8181(98)00040-X, 1998.

Pauler, C. M., Isselstein, J., Suter, M., Berard, J., Braunbeck, T., and Schneider, M. K.: Choosy grazers: Influence of plant traits on forage selection by three cattle breeds, Functional Ecology, 34, 980–992, https://doi.org/10.1111/1365-2435.13542, 2020.

Pei, Y., Dong, J., Zhang, Y., Yuan, W., Doughty, R., Yang, J., Zhou, D., Zhang, L., and Xiao, X.: Evolution of light use efficiency models: Improvement, uncertainties, and implications, Agricultural and Forest Meteorology, 317, 108 905, https://doi.org/10.1016/j.agrformet.2022.108905, 2022.

Petermann, J. S. and Buzhdygan, O. Y.: Grassland biodiversity, Current Biology, 31, R1195–R1201, https://doi.org/10.1016/j.cub.2021.06.060, 2021.

Prati, D., Goßner, M., and Neff, F.: Leaf traits of most abundant plant species from all EPs, 2017/2018, https://www.bexis.uni-jena.de/ddm/data/Showdata/24807?version=2, dataset ID: 24807, 2021.

Pulungan, M. A., Suzuki, S., Gavina, M. K. A., Tubay, J. M., Ito, H., Nii, M., Ichinose, G., Okabe, T., Ishida, A., Shiyomi, M., Togashi, T., Yoshimura, J., and Morita, S.: Grazing enhances species diversity in grassland communities, Scientific Reports, 9, https://doi.org/10.1038/s41598-019-47635-1, 2019.

Pärtel, M., Bruun, H., and Sammul, M.: Biodiversity in temperate European grasslands: origin and conservation, in: Integrating efficient grassland farming and biodiversity: Proceedings of the 13th international occasional symposium of the European grassland federation, vol. 10 of *Grassland Science in Europe*, pp. 1–14, 2005.

Riedo, M., Grub, A., Rosset, M., and Fuhrer, J.: A pasture simulation model for dry matter production, and fluxes of carbon, nitrogen, water and energy, Ecological Modelling, 105, 141–183, https://doi.org/10.1016/S0304-3800(97)00110-5, 1998.

https://doi.org/10.5194/egusphere-2024-3798
Preprint. Discussion started: 17 December 2024

Rolinski, S., Müller, C., Heinke, J., Weindl, I., Biewald, A., Bodirsky, B. L., Bondeau, A., Boons-Prins, E. R., Bouwman, A. F., Leffelaar, P. A., Te Roller, J. A., Schaphoff, S., and Thonicke, K.: Modeling vegetation and carbon dynamics of managed grasslands at the global scale with LPJmL 3.6, Geoscientific Model Development, 11, 429–451, https://doi.org/10.5194/gmd-11-429-2018, 2018.

Schapendonk, A. H. C. M., Stol, W., van Kraalingen, D. W. G., and Bouman, B. A. M.: LINGRA, a sink/source model to simulate grassland productivity in Europe, European Journal of Agronomy, 9, 87–100, https://doi.org/10.1016/S1161-0301(98)00027-6, 1998.

Schils, R. L. M., Newell Price, P., Klaus, V., Tonn, B., Hejduk, S., Stypinski, P., Hiron, M., Fernández, P., Ravetto Enri, S., Lellei-Kovács, E., Annett, N., Markovic, B., Lively, F., Ten Berge, H., Smith, K., Forster-Brown, C., Jones, M., Buchmann, N., Janicka, M., Fernandez, J., Rankin, J., McConnell, D., Aubry, A., and Korevaar, H.: European permanent grasslands mainly threatened by abandonment, heat and drought, and conversion to temporary grassland, https://doi.org/10.3929/ETHZ-B-000448642, 2020.

Schroeder-Georgi, T., Wirth, C., Nadrowski, K., Meyer, S. T., Mommer, L., and Weigelt, A.: From pots to plots: hierarchical trait-based prediction of plant performance in a mesic grassland, Journal of Ecology, 104, 206–218, https://doi.org/10.1111/1365-2745.12489, 2016.

Schöning, I.: Soil carbon and nitrogen concentrations - soil sampling campaign 2021, all experimental plots (EPs), 0-10 cm, https://www.bexis.uni-jena.de/ddm/data/Showdata/31210?version=13, dataset ID: 31210, 2023.

Schöning, I., Klötzing, T., Apostolakis, A., Trumbore, S., and Schrumpf, M.: MinSoil 2017 - Soil Carbon and Nitrogen Concentrations, https://www.bexis.uni-jena.de/ddm/data/Showdata/23846?version=10, dataset ID: 23846, 2021a.

Schöning, I., Solly, E., Klötzing, T., Trumbore, S., and Schrumpf, M.: MinSoil 2011 - Soil Carbon and Nitrogen Concentrations, https://www.bexis.uni-jena.de/ddm/data/Showdata/14446?version=19, dataset ID: 14446, 2021b.

Schöning, I., Solly, E., Klötzing, T., Trumbore, S., and Schrumpf, M.: MinSoil 2011 - Soil Texture, https://www.bexis.uni-jena.de/ddm/data/Showdata/14686?version=10, dataset ID: 14686, 2021c.

Schöning, I., Solly, E., Klötzing, T., Trumbore, S., and Schrumpf, M.: MinSoil 2011 - Soil Bulk Density and Carbon and Nitrogen stocks, https://www.bexis.uni-jena.de/ddm/data/Showdata/17086?version=4, dataset ID: 17086, 2021d.

Schöning, I., Trumbore, S., Schrumpf, M., Klötzing, T., and Gan, H. Y.: MinSoil 2014 - Soil Carbon and Nitrogen Concentrations, https://www.bexis.uni-jena.de/ddm/data/Showdata/18787?version=6, dataset ID: 18787, 2021e.

Siehoff, S., Lennartz, G., Heilburg, I. C., Roß-Nickoll, M., Ratte, H. T., and Preuss, T. G.: Process-based modeling of grassland dynamics built on ecological indicator values for land use, Ecological Modelling, 222, 3854–3868, https://doi.org/10.1016/j.ecolmodel.2011.10.003, 2011.

Silva, G. P., Fialho, C. A., Carvalho, L. R., Fonseca, L., Carvalho, P. C. F., Bremm, C., and Da Silva, S. C.: Sward structure and short-term herbage intake in Arachis pintoi cv. Belmonte subjected to varying intensities of grazing, The Journal of Agricultural Science, 156, 92–99, https://doi.org/10.1017/S0021859617000855, 2018.

Taubert, F., Frank, K., and Huth, A.: A review of grassland models in the biofuel context, Ecological Modelling, 245, 84–93, https://doi.org/10.1016/j.ecolmodel.2012.04.007, 2012.

Van Der Heijden, M. G. A., Martin, F. M., Selosse, M., and Sanders, I. R.: Mycorrhizal ecology and evolution: the past, the present, and the future, New Phytologist, 205, 1406–1423, https://doi.org/10.1111/nph.13288, 2015.

Van Oijen, M., Bellocchi, G., and Höglind, M.: Effects of Climate Change on Grassland Biodiversity and Productivity: The Need for a Diversity of Models, Agronomy, 8, 14, https://doi.org/10.3390/agronomy8020014, 2018.

Van Oijen, M., Barcza, Z., Confalonieri, R., Korhonen, P., Kröel-Dulay, G., Lellei-Kovács, E., Louarn, G., Louault, F., Martin, R., Moulin, T., Movedi, E., Picon-Cochard, C., Rolinski, S., Viovy, N., Wirth, S. B., and Bellocchi, G.: Incorporating Biodiversity into Biogeo-

https://doi.org/10.5194/egusphere-2024-3798
Preprint. Discussion started: 17 December 2024

chemistry Models to Improve Prediction of Ecosystem Services in Temperate Grasslands: Review and Roadmap, Agronomy, 10, 259, https://doi.org/10.3390/agronomy10020259, 2020.

Vogt, J., Weisser, W., Ayasse, M., Fischer, M., Schumacher, U., Schreiber, C., Lauterbach, R., Franke, A., Ostrowski, A., Teuscher, M., and Pompe, S.: Grassland management parameter as input data for a computer model based on interview data of the Biodiversity Exploratories project, https://www.bexis.uni-jena.de/ddm/data/Showdata/31715?version=9, dataset ID: 31715, 2024.

Wang, D.: MODIS/Terra+Aqua Photosynthetically Active Radiation Daily/3-Hour L3 Global 0.05Deg CMG V061, https://doi.org/10.5067/MODIS/MCD18C2.061, nASA EOSDIS Land Processes Distributed Active Archive Center. Accessed on 09.03.2023, 2021.

Watson, D. J.: Comparative Physiological Studies on the Growth of Field Crops: I. Variation in Net Assimilation Rate and Leaf Area between Species and Varieties, and within and between Years, Annals of Botany, 11, 41–76, https://doi.org/10.1093/oxfordjournals.aob.a083148, 1947.

Went, F.: The effect of temperature on plant growth, Annual Review of Plant Physiology, 4, 347–362, https://doi.org/10.1146/annurev.pp.04.060153.002023, 1953.

Westoby, M., Falster, D. S., Moles, A. T., Vesk, P. A., and Wright, I. J.: Plant ecological strategies: some leading dimensions of variation between species, Annual review of ecology and systematics, 33, 125–159, https://doi.org/10.1146/annurev.ecolsys.33.010802.150452, 2002.

Wilson, J. B., Peet, R. K., Dengler, J., and Pärtel, M.: Plant species richness: the world records, Journal of Vegetation Science, 23, 796–802, https://doi.org/10.1111/j.1654-1103.2012.01400.x, 2012.

Wirth, S. B., Poyda, A., Taube, F., Tietjen, B., Müller, C., Thonicke, K., Linstädter, A., Behn, K., Schaphoff, S., von Bloh, W., and Rolinski, S.: Connecting competitor, stress-tolerator and ruderal (CSR) theory and Lund Potsdam Jena managed Land 5 (LPJmL 5) to assess the role of environmental conditions, management and functional diversity for grassland ecosystem functions, Biogeosciences, 21, 381–410, https://doi.org/10.5194/bg-21-381-2024, 2024.

Wright, G. C., Hubick, K. T., Farquhar, G. D., and Rao, R. N.: Genetic and environmental variation in transpiration efficiency and its correlation with carbon isotope discrimination and specific leaf area in peanut, in: Stable isotopes and plant carbon-water relations, pp. 247–267, Elsevier, 1993.

Wright, I. J., Reich, P. B., Westoby, M., Ackerly, D. D., Baruch, Z., Bongers, F., Cavender-Bares, J., Chapin, T., Cornelissen, J. H. C., Diemer, M., Flexas, J., Garnier, E., Groom, P. K., Gulias, J., Hikosaka, K., Lamont, B. B., Lee, T., Lee, W., Lusk, C., Midgley, J. J., Navas, M.-L., Niinemets, Ü., Oleksyn, J., Osada, N., Poorter, H., Poot, P., Prior, L., Pyankov, V. I., Roumet, C., Thomas, S. C., Tjoelker, M. G., Veneklaas, E. J., and Villar, R.: The worldwide leaf economics spectrum, Nature, 428, 821–827, https://doi.org/10.1038/nature02403, 2004.

Wöllauer, S., Hänsel, F., Nauss, T., and Forteva, S.: Climate data - Time Series Web Interface, https://www.bexis.uni-jena.de/tcd/PublicClimateData/, dataset ID: 19007, 2023.

Zhang, L., Li, Y., Bai, W., Lambers, H., and Zhang, W.-H.: Morphological and physiological traits of dominant plant species in response to mowing in a temperate steppe, Ecological Applications, 33, e2863, https://doi.org/10.1002/eap.2863, 2023.